

# FINAL REPORT

## Metagenomic analysis of ADS dolphin *Hunter*

A/Prof Luciana Moller and Dr Jonathan Sandoval-Castillo  
College of Science and Engineering, Flinders University

August 2022

### Summary

Dolphins are sentinel species for the health of coastal environments, and those living near major cities are particularly vulnerable to environmental stressors. In recent decades, there has been an increase in the incidence and expansion of infectious diseases in these animals around the world. In Adelaide, about 40 Indo-Pacific bottlenose dolphins (*Tursiops aduncus*) are residents to the Port River estuary, which is part of the Adelaide Dolphin Sanctuary (ADS).

The estuary has great ecological significance, but it is also highly urbanised and industrialised. In recent years, concerns by the public, scientists and the government have risen about the health of the ADS dolphins, with several animals disappearing or dying. In 2021, a resident male dolphin, *named* Hunter, was euthanased on welfare grounds due to its severely ill condition. To aid in the investigation of its disease status, a shotgun metagenomics approach was applied to swab and tissue samples collected from the animal, and to water samples of the local environment. This was to assess microbial diversity and abundance in different dolphin body regions (integumentary, respiratory, digestive, sensory, lymphatic, reproductive, urinary, central nervous and circulatory systems), and in the seawater.

Bacteria were the most abundant taxa overall, followed by small representation of viruses, fungi and Archaea. Proteobacteria was extremely abundant in the ear sample, and abundant in the rectum, mouth, non-lesioned and lesioned skin, and the seawater. Bacteroidetes were very abundant in the kidney, and considerably abundant in the blowhole and one skin lesion. Firmicutes were dominant in the colon samples and abundant in the rectum, while Actinobacteria had high representation in the brain and heart. Chlamydiae also had a moderate contribution to the liver. Several microorganisms of pathogenic potential, particularly those associated with gastro-intestinal diseases, and including zoonotic agents, were identified. Bacteria associated with polluted environments were also observed in the dolphin skin.

The most abundant genera were *Vibrio*, *Photobacterium*, *Hydrobacter*, *Clostridium*, *Tenacibaculum*, *Arcobacter*, *Alcanivorax*, *Edwardsiella*, *Aureispira*, and *Psychrobacter*. The ear was dominated by the genus *Edwardsiella*, species *E. tarda*, while the kidney was largely represented by *Hydrobacter*. The distal colon and rectum were overrepresented by *Photobacterium damsela*, *Clostridium perfringens* and other Clostridia. The stomach was overly represented by *Candidatus Ichthyocystis hellenicum*. The liver had a high abundance of *Clostridium* and a moderate abundance of *Chlamydia*, which was identified as *C. abortus*. The lesioned skin was mainly composed of *Vibrio harveyi*, *V. genomosp.*, *Arcobacter*, *Aureispira* sp., and *Tenacibaculum ovolyticum*. The non-lesioned skin had a very different main microbial composition to the lesioned skin, with genera such as *Alcanivorax* and

*Sphingopyxis* present. The bacterial composition of the seawater was very different to the dolphin samples.

Among the viruses, retroviruses were the most abundant, followed by Phycodnaviridae (mostly in the seawater), Podoviridae, and Myoviridae. Papillomaviridae, represented by *T. truncatus* papillomavirus 6, was found in the rectum sample, and Poxviridae in the non-lesioned skin, but most of the viruses were represented by phages or retroviruses.

The metagenomic analysis showed major differences in the diversity and abundance of microbial taxa in the different body systems examined and the seawater. These differences corroborate the idea that distinct physiochemical conditions and disease status impact on animal microbiomes. The study represents the first comprehensive microbial inventory of a diseased ADS dolphin, and further analysis of the gene catalogue could include other non-microbial eukaryotes.

The study also demonstrates that shotgun metagenomics is a valuable tool for microbial and pathogen surveillance in marine mammals and estuarine environments. Additional studies on the microbial composition of ADS dolphins and their prey, and seawater in the Port River system, can assist with continued monitoring of disease agents pertinent to dolphins, other marine animals, and humans. Information from this study is important for the management of ill ADS dolphins, and for potentially mitigating risks to the local wildlife and the public.

## Introduction

Dolphins are long-lived, near-top predators that act as sentinels of the health of coastal ecosystems and potential bio-indicators of public health (Wells et al. 2004; Bossart 2011). Dolphins living near cities are vulnerable to various stressors, including habitat modification, pollution, harmful algal blooms, and emerging diseases (e.g., Van Bresse et al. 2009; Fire et al. 2011; Wang et al. 2017; Byard et al. 2020). Some of these impacts have recently led to dolphin morbidities and mortalities around the world (e.g., Fire et al. 2015; Kemper et al. 2016).

Adelaide is home to about 280 Indo-Pacific bottlenose dolphins (*Tursiops aduncus*), with about 40 residents to the Port River estuary (Zanardo et al. 2016; Bossley et al. 2017). The estuary is a complex environment with saltmarshes, mangroves, and seagrasses, and is inhabited by a range of marine species (Environment Protection Authority (EPA), 2005). In 2005 the government of South Australia (the government) declared the area as the ADS due to concerns about the dolphins' welfare (ADS Management Plan (DEW, 2008)). The Sanctuary aims to protect the dolphins and its habitats. Apart from its ecological significance, the estuary has important economic value to South Australia due its large industrial hub, port facilities and urbanised areas. These developments have affected its health due to a range of activities, including channel dredging, aquatic vegetation removal, wastewater discharge, thermal pollution, and stormwater flow (EPA, 2003).

After ADS implementation, several strategies were adopted to mitigate impacts, particularly around water quality (EPA, 2003). However, concerns have again risen in recent years about the dolphins' health, with several disappearing (presumed dead) and others dying from disease (Tomo and Kemper 2021; ADS Investigation Interim Report, 23/11/21 (DEW, 2021)). In 2021 several juveniles and sub-adults became ill and disappeared or died within a few months (DEW, 2021). Community and government concerns led the former Minister for the Environment and Water (DEW) to call for an investigation into the health of the dolphins. Results from a range of tests (blood, contaminants, bacterial cultures, PCR for targeted pathogens, serology, and bio-toxins) on three recovered carcasses and one sick animal (captured for disentanglement of fishing line and hooks) were inconclusive as to the cause of deaths and commonalities (Post-mortem reports; DEW, 2021). Shortly after, another ill animal, a juvenile male named *Hunter*, was euthanased on welfare grounds due to its rapidly deteriorating body condition. Post-mortem analyses of this animal revealed various opportunistic infections and enteropathy, with microbial cultures suggestive of intestinal dysbiosis (Post-mortem report; DEW, 2021). Given the body's freshness, several samples were collected for metagenomic analyses of the dolphin's microbiome. Given that most microbes (>98%) cannot be readily culture under laboratory conditions (Stewart 2012), next-generation sequencing technologies are becoming increasingly popular for these studies (e.g., Godoy-Vitorino et al. 2016; Robles-Malagamba et al. 2020).

The microbiome comprises all microorganisms, including pathogens, which are found both within and on organisms. Most microbes contribute positively to the host-microbe ecosystem by providing various services, but microbiome imbalance can lead to loss of beneficial functions or infections by pathogens. Information on dolphin microbiomes are critical for understanding their health status, the epidemiology of populations, and for potentially identifying changes to the health of marine and coastal ecosystems (e.g., Godoy-Vitorino et al. 2016; Robles-Malagamba et al. 2020; Wan et al. 2021). In addition, knowledge about the

exposure of dolphin populations to pathogens and potential risks of transmission to humans are desirable when capturing and treating ill animals (Godoy-Vitorino et al. 2016).

Recently, there has been a rapid increase in the incidence and expansion of infectious diseases in cetaceans around the world, particularly coastal dolphins, caused by viruses, bacteria and parasites, some of which are associated with high mortalities, reduced reproductive success, or an increase in the virulence of other diseases (e.g., Van Bresseem et al. 2009; Di Guardo et al. 2018; Sanderson and Alexander 2020). Here, shotgun metagenomics is used to assess the microbial diversity and abundance in samples of the dolphin *Hunter*, with a focus on bacteria and DNA viruses of pathogenic potential. Results from this study will contribute to the investigation into the health status of the ADS dolphins.

## Material and methods

### *Collection of samples for metagenomics*

The dolphin sampled for the study was a known juvenile male (*Hunter*, 6 yrs old) resident to the ADS. The animal was euthanised on welfare grounds around Garden Island on 22/10/21 by a referring veterinarian from ZoosSA after his condition deteriorated rapidly in the previous weeks (Post-mortem, pathology report 21-02676, University of Adelaide, hereafter the PM report). Swab (sterile nylon fibre, FLOQSwabs, Copan) samples of external body regions and orifices were collected on site within 20 min of the animal's death, and swab and tissue samples of internal organs were collected during post-mortem examination at the Veterinary Diagnostic Laboratory (School of Animal and Veterinary Science, Adelaide University) within 4 hrs of the animal's death. Samples included representatives of the integumentary, respiratory, digestive, sensory, lymphatic, reproductive, urinary, central nervous and circulatory systems (**Table S1**). All samples were stored in sterile tubes filled with RNAlater (Qiagen), and frozen (ice while in the field, -20°C in the lab at Adelaide University, and -80°C on return to Flinders University) until analyses. Seawater for analysis was also collected from Garden Island boat ramp, adjacent to where the animal was located prior to euthanasia, and again at Garden Island and Snowden Beach approximately 1 month later. 1L of seawater was collected in a bottle at each time and filtered through a Sterivex (Merck) 0.22 µm filter unit on site and frozen until analysis (ice while in the field, and -80°C on return to Flinders University).

### *DNA extraction and quality control*

DNA was extracted from samples at the Molecular Ecology Laboratory (College of Science and Engineering, Flinders University) using a DNeasy blood & tissue kit (Qiagen) with a pre-treatment protocol for gram-positive bacteria as outlined in the kit's manual. Prior to extraction, tissue samples (approximately 3-5mm<sup>3</sup>) and the Sterivex filter were cut into smaller pieces using sterile blades, while swabs were immersed directly into the lysis buffer.

After extraction, DNA quantity and quality was assessed using a Qubit 2.0 fluorometer (Life Technologies), NanoDrop 1000 spectrophotometer (Thermo Scientific) and agarose gel electrophoresis. Samples that passed quality control were sent for sequencing at Novogene using a metagenomics whole genome shotgun (mWGS) approach (**Table S1**). Five samples that failed quality control were not sent for sequencing.

### *Whole genome shotgun sequencing*

Whole genome shotgun sequencing at Novogene involved initial sample quality control, library construction, library quality control, and sequencing on an Illumina platform. Information below is based on Novogene's workflow and reporting protocols.

Sample quality control included quantification and qualification with a Qubit fluorometer, NanoDrop spectrophotometer and agarose gel electrophoresis. All samples were deemed of acceptable quality for sequencing by Novogene (data not shown). For library construction, genomic DNA was randomly sheared into short fragments. The fragments were then end repaired, A-tailed and ligated with an Illumina adapter. Fragments with the adapters were PCR amplified, size selected, and then purified. The quantified (via Qubit and real-time PCR) and size inspected (via Bioanalyser) library was pooled and paired-end (150bp) sequenced on a NovaSeq 6000 Illumina platform, to approximately 12 Gb of raw data per sample.

### ***Bioinformatics of metagenomic data***

Novogene bioinformatics included initial data quality control, metagenome assembly, gene prediction, and taxonomy annotation.

Data quality control after sequencing involved filtering of low-quality data and the host genome from the raw data to ensure accuracy and reliability for analyses (**Table S2**). The protocol included: 1) trimming of low-quality bases (Q-value  $\leq 38$ ) which exceed 40 bp; 2) trimming of reads which contain N nucleotides over 10bp; 3) trimming of reads which overlapped with adapter over 15bp; 4) and for the dolphin samples, minimalizing the host DNA (using an in-house, chromosome-length scaffolded, *Tursiops aduncus* reference genome, Batley et al. unpublished) using Bowtie2 (Langmead and Salzberg 2012).

The clean data were used for metagenome assembly of each sample (**Table S3**). Samples were initially assembled using MEGAHIT (Li et al. 2015). Scaffolds were cut off at 'N' to get fragment without 'N'; these are referred to as Scaffigs, which are continuous sequences within scaffolds (Mende et al. 2012, Nielsen et al. 2014). The clean data were then mapped to the assembled Scaffigs using Bowtie2. After, unutilised paired-end reads of each sample were combined for mixed assembly to investigate low-abundance species. The scaffigs of each sample and the mixed assembly were then trimmed if  $< 500\text{bp}$  (Nielsen et al. 2014). The remaining scaffigs were finally used for gene prediction with open reading frames (ORF).

ORF prediction was done with MetaGeneMark based on scaffigs ( $\geq 500\text{bp}$ ) assembled by both single and mixed samples (Li et al. 2014). ORFs  $< 100\text{nt}$  were trimmed (Nielsen et al. 2014), and remaining ORFs were dereplicated by CD-HIT (Li et al. 2006) (parameters: -c 0.95, -G 0, -aS 0.9, -g 1, -d 0; Zeller et al. 2014) to develop the gene catalogue, with the longest ORF chosen as the representative gene, or unigene. Clean data were then mapped to the gene catalogue using Bowtie2 to estimate abundance. Abundance was calculated based on the total number of mapped reads and the gene length, with formula:  $Gk = rkLk \cdot \sum ni = IriLi$ , where  $r$  denotes the number of mapped reads and  $L$  denotes the length of a gene (Zeller et al. 2014). Downstream analyses were performed based on the abundance of the gene catalogues (**Table S4**).

Novogene's taxonomy annotation ensued after gene prediction. To annotate each metagenomic homolog, metagenomic reads were compared to the micro-NR database, which is a database of taxonomically informative gene families, using MEGAN, with an e-value threshold of  $1e^{-03}$ . After checking Novogene results in-house for multiple annotated genes at the lowest taxonomic levels (genus and/or species), it appeared that the relaxed threshold used by their pipeline led to several false positives (data not shown).

To improve Novogene's taxonomic annotation, viruses, and other taxa with e-values  $\geq 1e^{-10}$  and  $\geq 1e^{-20}$ , respectively, were removed. After, genes were re-annotated in-house against the National Center for Biotechnology Information (NCBI) NR database, using DIAMOND (Buchfink et al. 2021). Any gene that was annotated consistently to non-microbial eukaryotes (including Odontoceti and Teleostei) with higher similarity and lower e-values than its corresponding annotation in the microNR database, was removed. Microbial eukaryotes included here are limited to fungi.

For each taxonomic level, the 10 most common taxa from each sample were used to create stacked barplots of relative proportions (12 for virus-only plots). The most common taxa were also used to create a heat map of species abundance (identified species within the 10

most common genera). An interactive Krona chart was also created for visualising relative abundances of taxonomic groups at different hierarchical levels for each sample (Ondov et al. 2011).

## Results

### *Gene numbers in the different body systems and in the dolphin core microbiome*

Common and distinctive **genes** identified in the samples of dolphin *Hunter* are presented in a Venn diagram (**Figure 1**). The integumentary system, represented by the skin samples, including lesioned and non-lesioned skin, showed the greatest number of unique genes, followed by the respiratory system, represented by the blowhole and lung, and the digestive system, represented by the mouth, stomach, colon, rectum, and liver samples. The lymphatic system, represented by the spleen did not show any unique genes, while the central nervous system, represented by the brain, and the sensory system, represented by the ear, showed a small number of unique genes. The **core microbiome** of dolphin *Hunter* based on the available samples was represented by 1,433 unique genes.

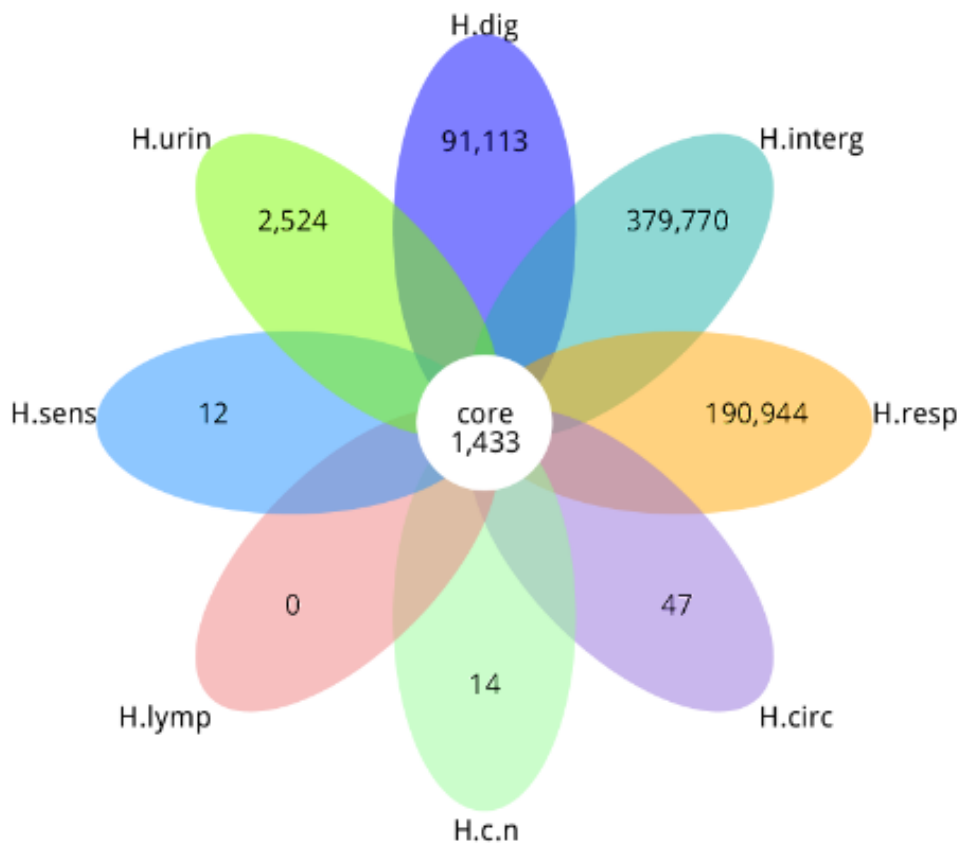


**Figure 1.** Number of common and peculiar genes among body systems and the core microbiome of dolphin *Hunter* as revealed by metagenomic sequencing of 18 samples. **Notes:** H. = Hunter; dig = digestive; interg = integumentary; resp = respiratory; circ = circulatory; c.n = central nervous;lymp = lymphatic; sens = sensory, urin = urinary.

### Correlations between the dolphin samples and the seawater

The correlation in the predicted genes between different samples of dolphin *Hunter* and the seawater is indicated in **Figure 2**. Strong positive correlations were observed between the lung, spleen, brain, liver, and heart, which comprised all the tissue samples, except the kidney. Moderate negative correlations were observed between the non-lesioned skin, the blowhole, and the seawater sample. Most correlations between samples were slightly negative to positive. All the correlations between the dolphin samples and the seawater were negative.

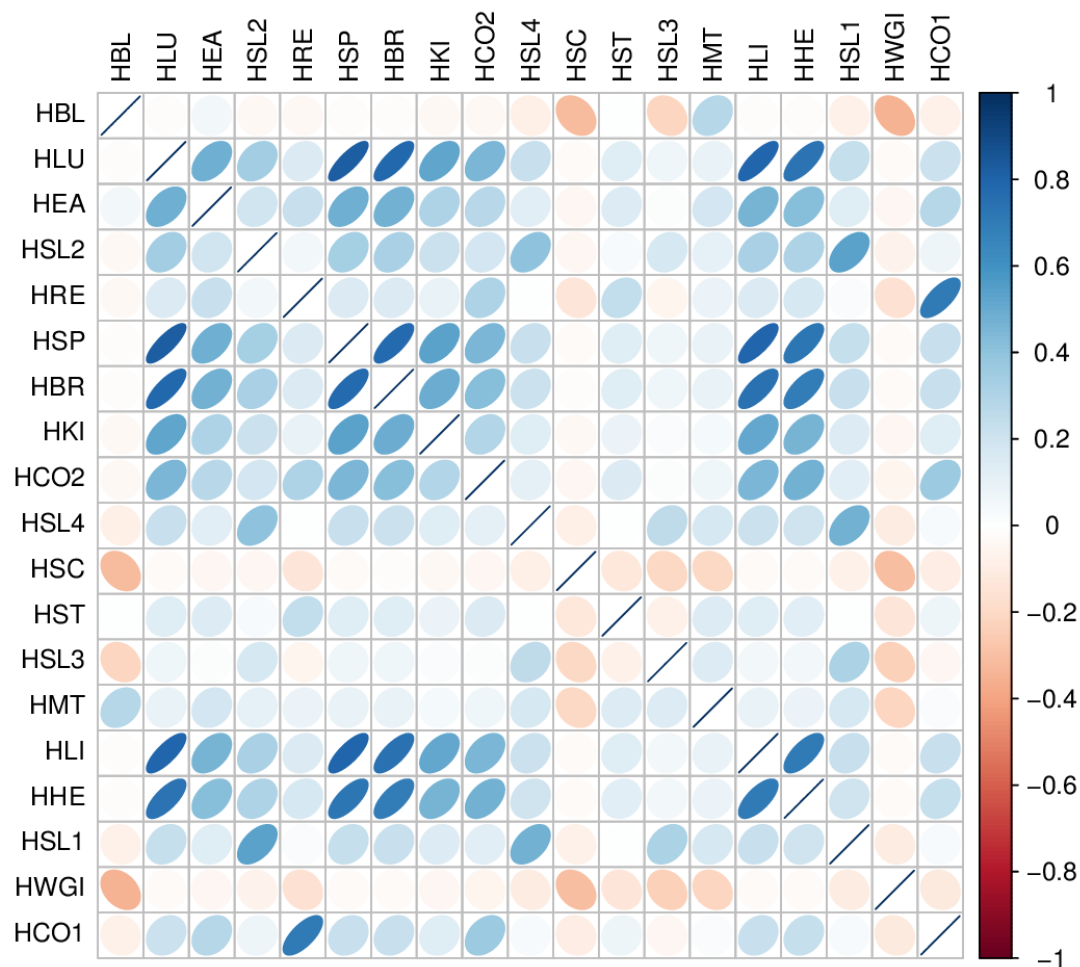


**Figure 2.** Correlation of predicted genes between the dolphin samples and the seawater. **Note:** Blue bubbles mean positive correlation, while red bubbles mean negative correlation, with deeper colours denoting greater association. **Notes:** HBL = blowhole; HLU = lung; HEA = left ear; HSL2 = skin lesion 2; HRE = rectum; HSP = spleen; HBR = brain; HKI = kidney; HCO2 = proximal colon; HSL4 = skin lesion 4; HSC = non-lesioned skin; HST = stomach; HSL3 = skin lesion 3; HMT = mouth; HLI = liver; HHE = heart; HSL1 = skin lesion 1; HWGI = seawater (Garden Island); HCO1 = distal colon.

**Microbial taxonomic diversity and relative abundance in the dolphin samples and the seawater**

Bacteria (87.02%) had the largest representation overall, followed by DNA viruses (and retroviruses) (0.35%), microbial eukaryotes (0.21%) and Archaea (0.03%), with a percentage remaining unclassified (14.14%).

The most abundant **phylum** across samples was Proteobacteria, followed Bacteroidetes and Firmicutes (**Figure 3**). Proteobacteria was extremely abundant in the ear sample (~88%), and abundant (> 50%) in the rectum, mouth, non-lesioned skin, two of the skin lesions (SL1 and SL2), and the seawater. Bacteroidetes were extremely abundant in the kidney sample (~98%), and considerably abundant (~50%) in the blowhole and one of the skin lesions (SL3). Firmicutes were dominant in the colon samples (~65-85%) and abundant in the rectum (~43%). Actinobacteria had a relatively high representation in the brain and heart (~25-30%). Chlamydiae had a moderate contribution to the liver sample (~8%).

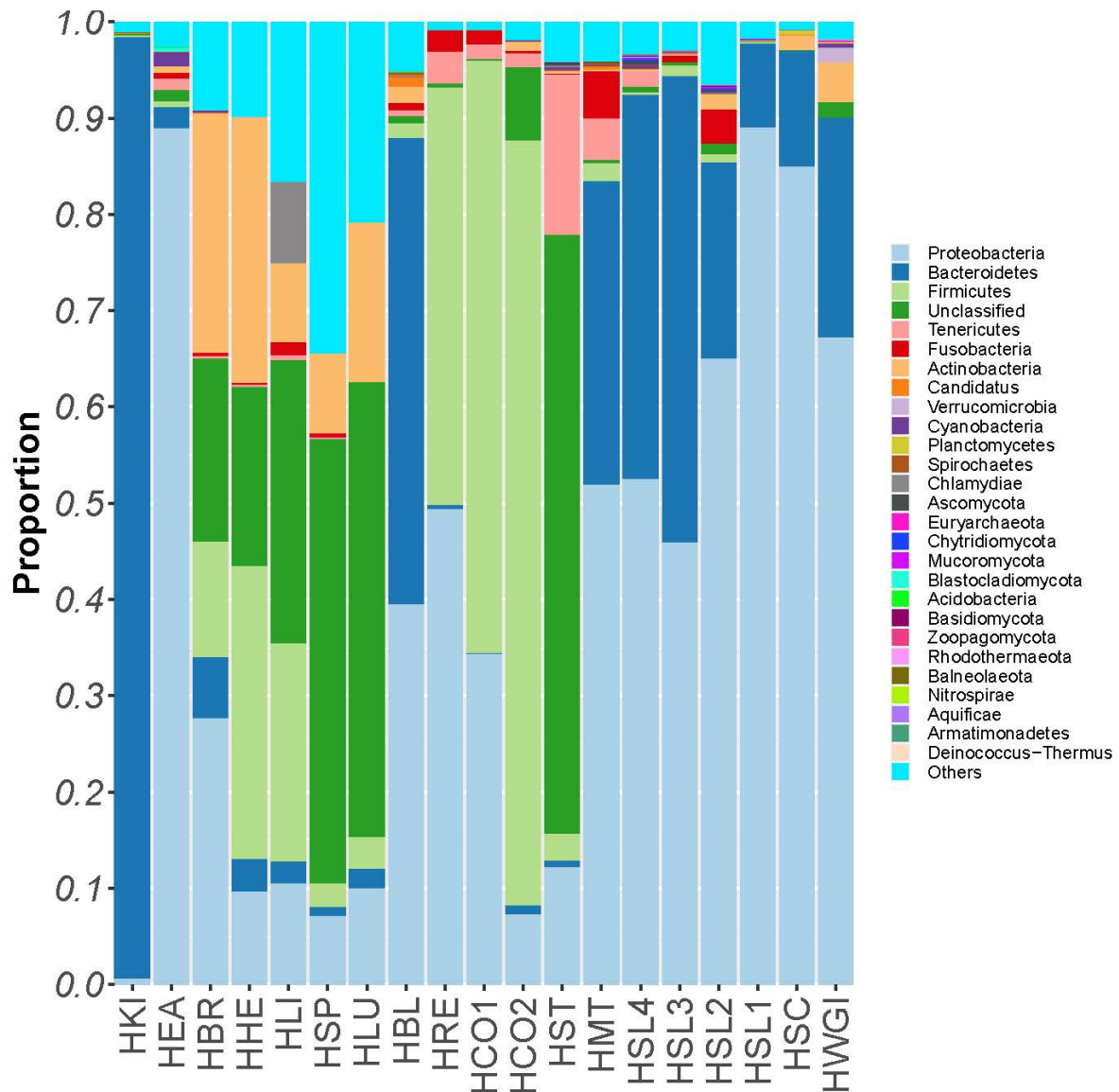


**Figure 3.** Relative abundance of the 10 most common taxa from each sample at the phylum level. Sample abbreviations as in Figure 2.

At the **genus** level, the 10 most abundant genera across samples were *Vibrio*, *Photobacterium*, *Hydrobacter*, *Clostridium*, *Tenacibaculum*, *Arcobacter*, *Alcanivorax*, *Edwardsiella*, *Aureispira*, and *Psychrobacter* (**Figure 4**). The ear was dominated by the genus *Edwardsiella* (~85%), while the kidney was largely represented by *Hydrobacter* (~50%). The distal colon and rectum were overrepresented by *Photobacterium* (~30-45%) and *Clostridium* (~25%). Two of the skin lesions had high proportions of *Vibrio* (~55-60%). Several genera among the top 10 of the lesioned skin were found in common (e.g., *Vibrio*, *Tenacibaculum*, *Arcobacter*), but not in the non-lesioned skin or the seawater. The spleen, lung, liver, brain, and heart had moderate to large proportions of beta retroviruses (~15-55%), with the last two also showing relatively high abundance of *Corynebacterium* (~16-23%). The liver had a relatively high abundance of *Clostridium* (~17%) and a moderate abundance of *Chlamydia* (~8%).

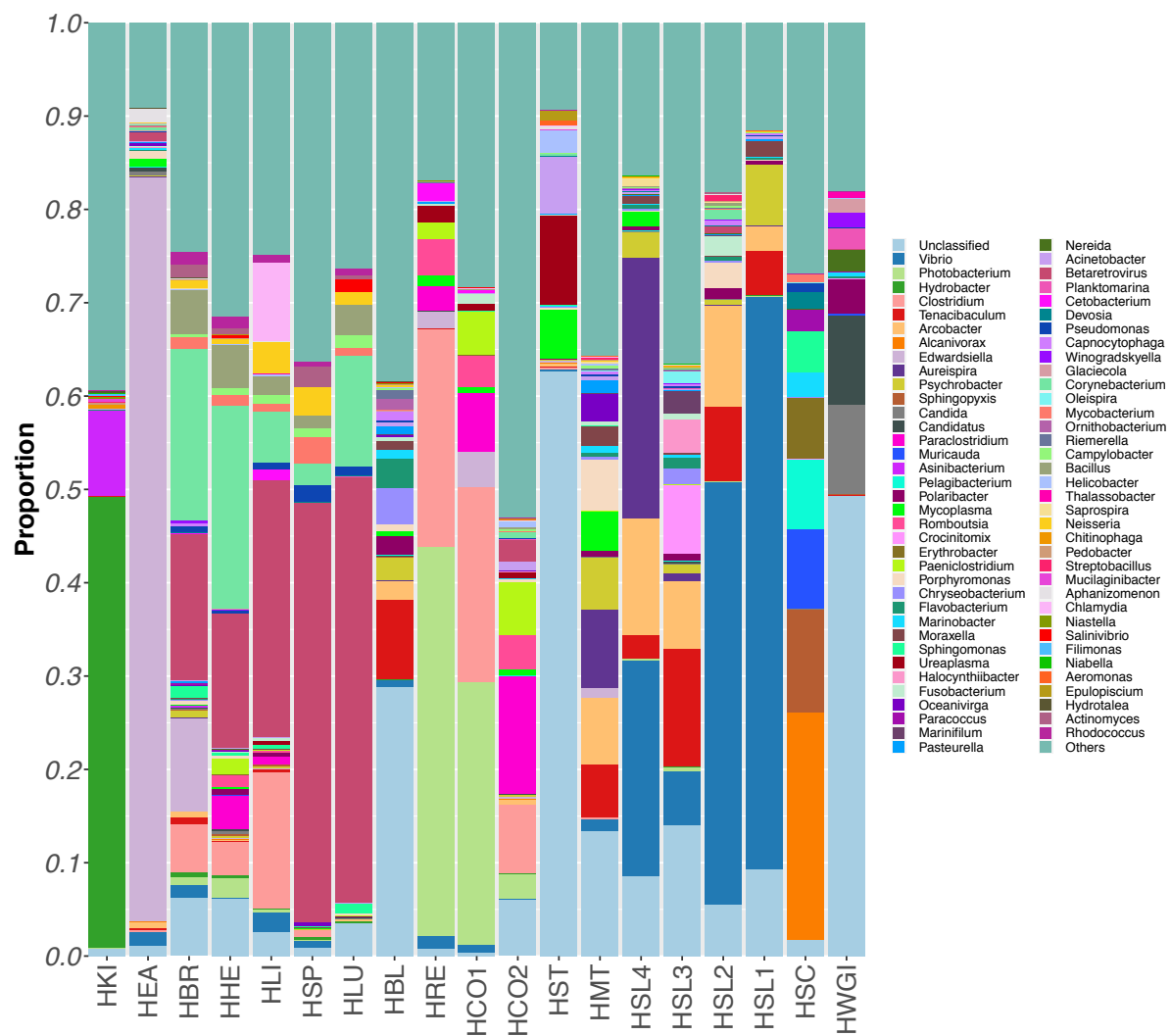


**Figure 4.** Relative abundance of the 10 most common taxa from each sample at the genus level. Sample abbreviations as in Figure 2.

Within the top 10 genera observed in each sample, several **species** were identified (**Figure 5**). The species *Edwardsiella tarda* was overrepresented in the ear (~65%), and *Hydrobacter penzbergensis* in the kidney (~47%). The rectum and distal colon were dominated by the species *Photobacterium damsela* (~26-40%) and *Clostridium perfringens* (~15%), while the proximal colon showed relatively high proportions of *Paraclostridium bifermentans* (~8%) and *Paenoclostridium sordellii* (~7%). The liver also showed high relative proportions of *C. perfringens* (~13%) and *Chlamydia abortus* (~8%), while the stomach had relatively large representation of *Acinetobacter baumannii* (~8%). The species *V. genomosp.* (~20%), *V. harveyi* (~12%) and *T. ovolyticum* (~10%) had relatively high combined representation in the lesioned skin.

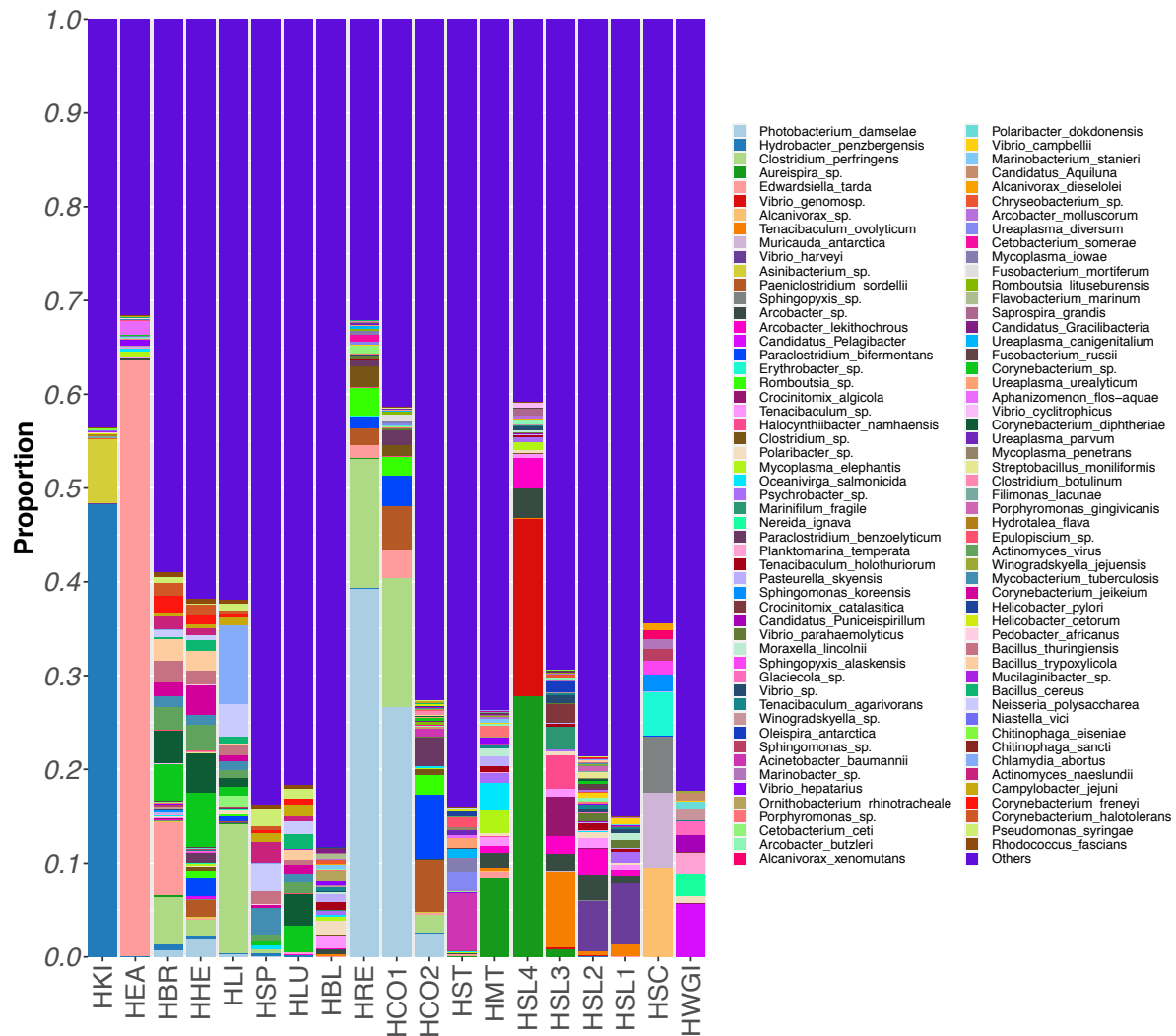


**Figure 5.** Relative abundance of identified species within the 10 most common genera from each sample. Sample abbreviations as in Figure 2.

The identified species (within the 10 top common genera) that were significantly different among the samples ( $p < 0.05$ ) are shown in a heatmap (Figure 6). The samples with the most differentiated frequency composition of species were represented by the non-lesioned skin (e.g. *Muricauda antarctica*, *Sphingopyxis alaskensis*, *Sphingomonas koreensis*), the seawater

(e.g. *Planktomarina temperata*, *Nereida ignava*) and skin lesion 3 (e.g. *Crocinitomix algicola*, *Halocynthiibacter namhaensis*, *T. ovolyticum*). Other species which were significantly more abundant in particular samples included *E. tarda* in the ear; *H. penzbergensis* in the kidney; *Ornithobacterium rhinotracheale* in the blowhole; *P. damsela*, *Clostridium* sp. and *Romboutsia* sp. in the rectum; *P. sordellii*, *Paraclostridium benzoelyticum* and *P. bifermentans* in the distal colon; *A. baumannii* in the stomach; *Oceanivirga salmonicida* and *Mycoplasma elephantis* in the mouth; *V. genomosp.* and *Aureispira* sp. in skin lesion 4; and *V. harveyi* in skin lesion 1. Some similarities in frequency composition can also be seen among the blowhole, mouth, and lesioned skin (e.g., *Tenacibaculum* spp., *Psychrobacter* sp., and *Moraxella lincolnii*), as well as between the rectum and distal colon (e.g. *P. damsela*, *C. perfringens*, *Romboutsia* sp., *P. bifermentans*, *Paraclostridium benzoelyticum*, *P. sordellii*, *V. parahaemolyticus*), and to a lesser extent to the proximal colon.

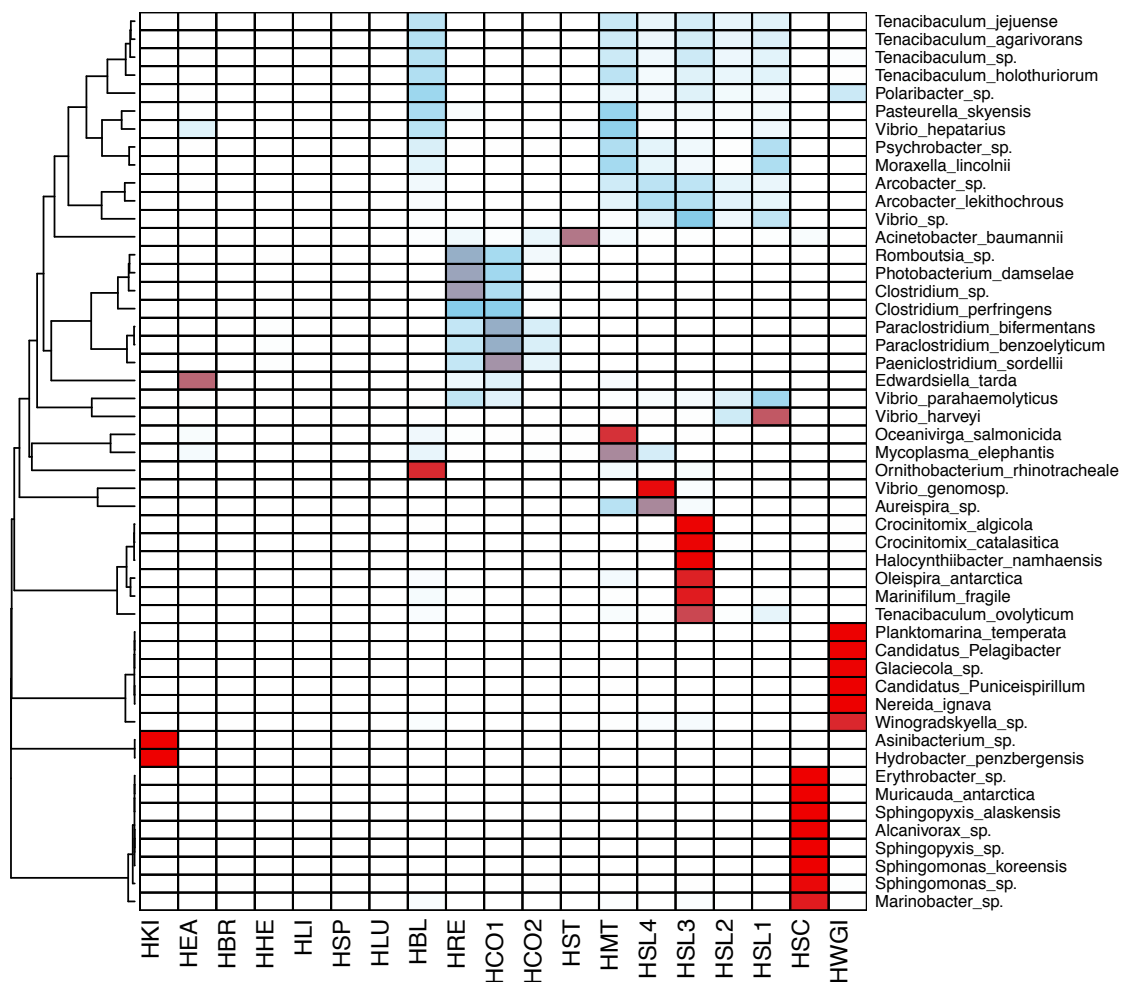


**Figure 6.** Heatmap depicting significantly different species identified within the 10 most common genera from each sample. Sample abbreviations as in Figure 2.

Although DNA **viruses** (and retroviruses) represented only a small proportion of the taxa identified, it is relative distribution across the samples, at family level, can be seen in **Figure 7**. Retroviruses were the most abundant, followed by Phycodnaviridae (mostly in the seawater), Podoviridae, and Myoviridae. Papillomaviridae showed moderate representation in the rectum sample, and Poxviridae had a small representation in the non-lesioned skin.

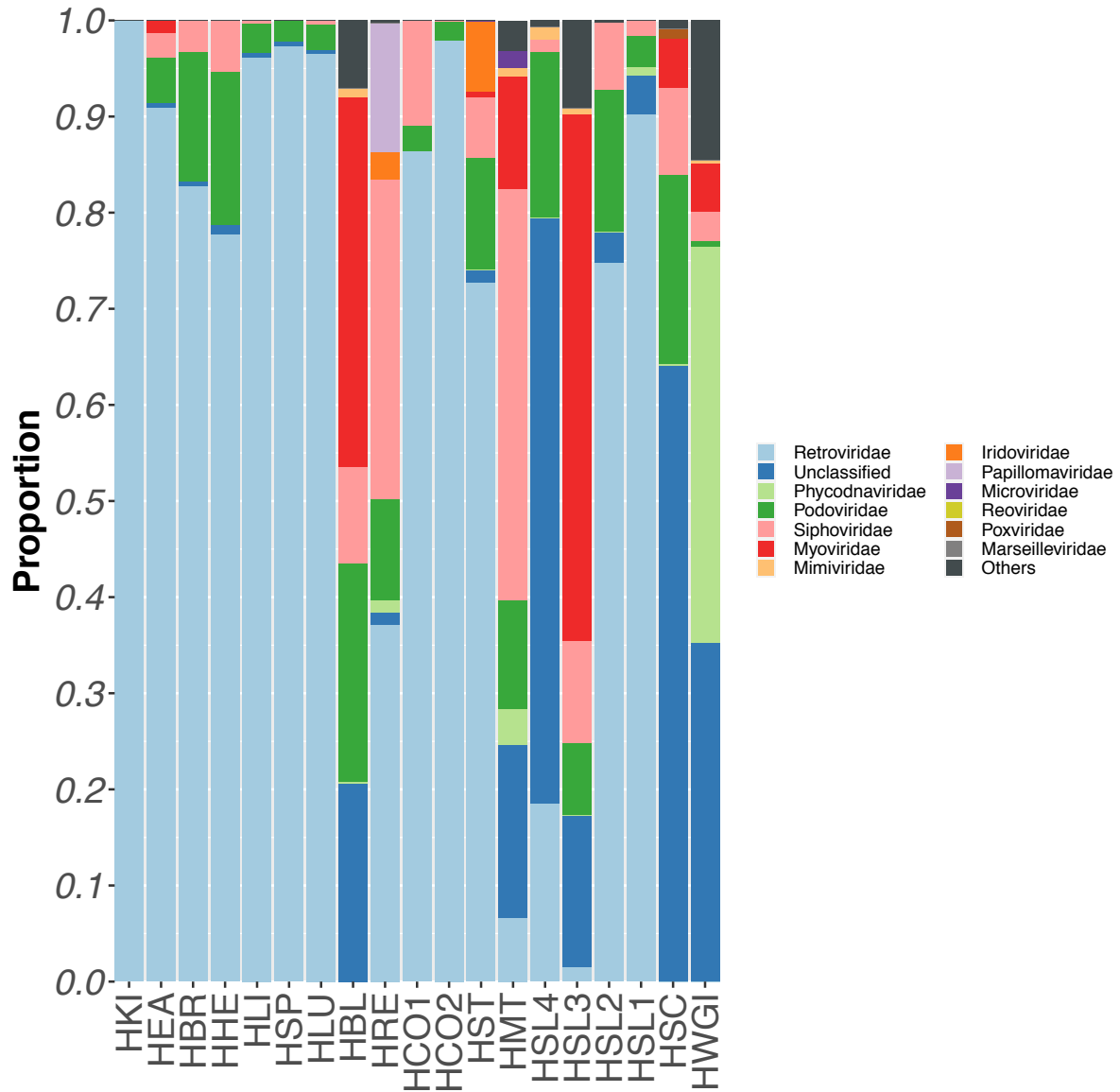


**Figure 7.** Relative abundance of the 12 most common viral taxa from each sample at the family level. Sample abbreviations as in Figure 2.

At the **species** level, most identified viruses were represented by phages (viruses that infect and replicate within bacteria and archaea) and retroviruses (RNA viruses that integrate into the host genome), with a few exceptions, such as *T. truncatus* papillomavirus 6 observed in the rectum sample, and lymphocystis, mainly in the mouth and stomach (Figure 8).

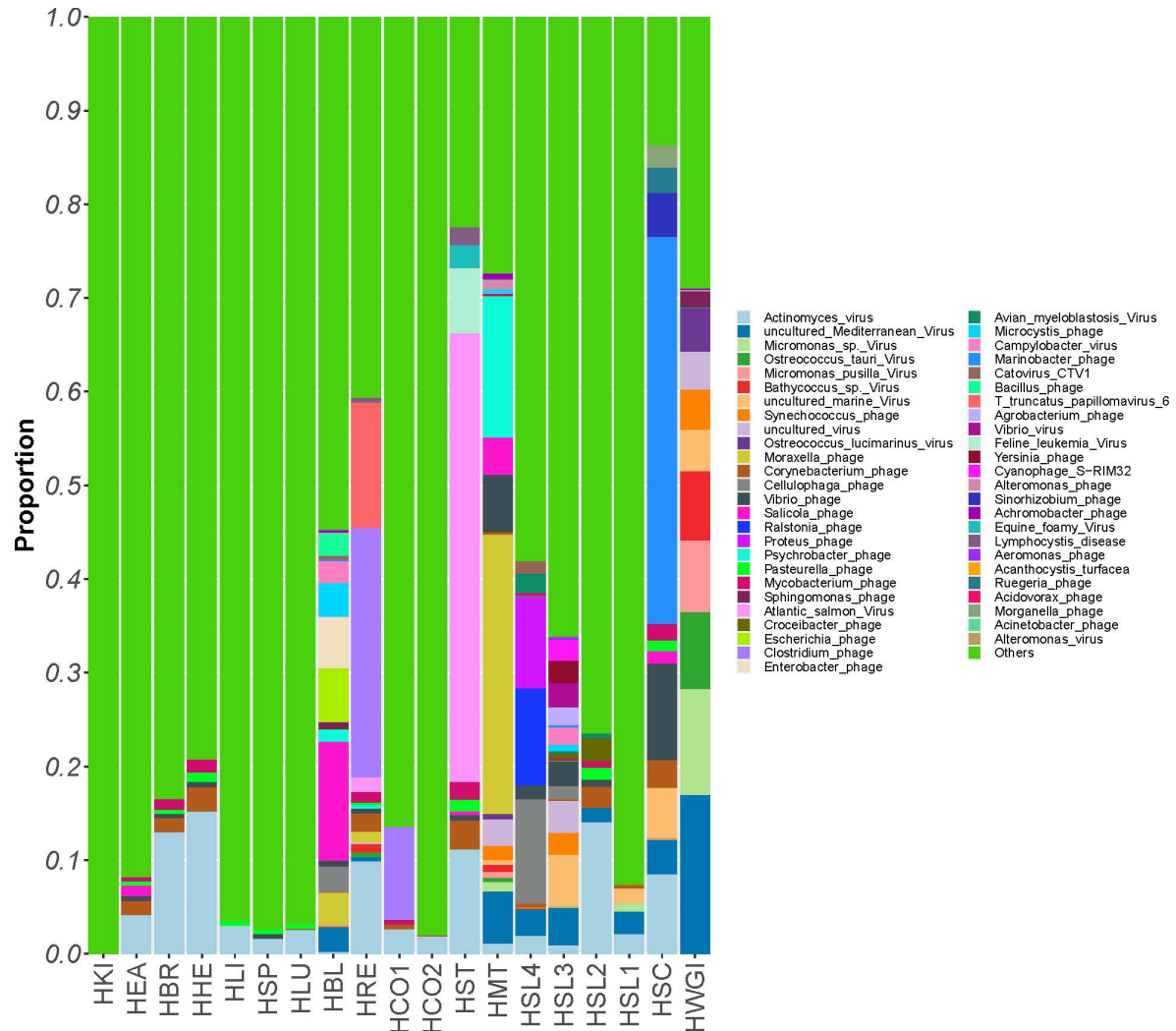


**Figure 8.** Relative abundance of the 12 most common viral taxa from each sample at the species level. Sample abbreviations as in Figure 2.

Further information about taxa diversity and abundance can be gained by exploring the Krona chart for each individual sample (Figures S1-S19).

The **kidney** was mainly characterized by Bacteroidetes of the family Chitinophagaceae (89%), with one species (*H. penzbergensis*) dominant in the sample (48%), followed *Asinibacterium* sp. (7%) (Figure S1).

The **ear** was dominated by Proteobacteria (89%), with one family (Hafniaceae) and species (*E. tarda*) contributing most sequences (63%) (**Figure S2**). Eukaryotes made up 2% of this sample, but only one fungal family was identified (Blastocladiaceae).

The **brain** had a high representation of Proteobacteria (34%), Actinobacteria (31%), Firmicutes (15%) and Bacteroidetes (8%) among the bacteria (81%) and of betaretroviruses (16%) among the viruses (19%) (**Figure S3**). Several species of the genus *Corynebacterium* were present, including *C. diphtheriae*. Other relatively abundant species identified included *E. tarda* (8%) and *C. perfringens* (5%). Some Bacilli species (e.g., *B. thuringiensis* and *B. trypoxylicola*) were also present. Note that *Mycobacterium tuberculosis* was identified in the sample (1%).

The **heart** had a large proportion of bacteria (81%) from the phyla Firmicutes (37%), Acinobacteria (34%), Proteobacteria (12%), and Bacteroidetes (4%), and of betaretroviruses (14%) among the viruses (18%) (**Figure S4**). Like the brain sample, several species of the genus *Corynebacterium* were present, including *C. diphtheriae* (4%). Several species of the class Clostridia, including *C. perfringens*, *P. sordellii*, *P. bifermentans*, *P. benzoelyticum*, as well as Bacilli (*B. cereus*, *B. thuringiensis*, and *B. trypoxylicola*) were present. Note that *M. tuberculosis* was also identified in this sample (1%).

The **liver** had a large representation of bacteria (71%) from the phyla Firmicutes (32%), Proteobacteria (15%), Chlamydiae (12%), and Actinobacteria (11%), and of betaretroviruses (27%) (**Figure S5**). *C. perfringens* (14%) and *C. abortus* (8%) were the identified species with highest contribution to the sample. It also showed *Neisseria polysaccharea*, *Vibrio* spp., *Cetobacterium ceti*, *C. diphtheriae*, and *B. thuringiensis* at 1-3% frequency each.

The **spleen** had a high representation of betaretroviruses (45%), and bacteria (54%) from the phyla Actinobacteria (15%) and Proteobacteria (13%), although a large proportion of bacteria (64%) remained unassigned (**Figure S6**). Species identified in the sample at  $\geq 3\%$  included *N. polysaccharea* (6%), *M. tuberculosis* (5%), *Actinomyces naeslundii* (4%), *Pseudomonas syringae* (3%), and *B. thuringiensis* (3%).

The **lung** had most of its bacterial composition from Actinobacteria (31%), Proteobacteria (19%) and Firmicutes (6%), and a large proportion of retroviruses (46%) (**Figure S7**). Some of the species identified at 1-3% abundance were *C. diphtheriae*, *B. cereus*, *C. jejuni*, *N. polysaccharea* and *P. syringae*.

The **blowhole** was mainly represented by bacteria, with Bacteroidetes comprising most of the sample (49%), followed by Proteobacteria (40%) (**Figure S8**). At genus level, *Tenacibaculum* (9%), *Chryseobacterium* (8%), *Psychrobacter* (3%), *Flavobacterium* (3%), *Polaribacter* (2%) and *Arcobacter* (2%) had relatively high representation among the bacteria. Only a few taxa were identified to the species level in this sample, including *O. rhinotracheale*, *P. skyensis* and *Tenacibaculum holothuriorum* (~1% each).

The **rectum** was mainly represented by bacteria of the phyla Proteobacteria (49%) and Firmicutes (43%) (**Figure S9**). The sample was overrepresented by a species of Vibrionaceae, *P. damsela* (39%). It also had a very large representation of Clostridia (43%), particularly *C. perfringens* (14%), but also *Romboutsia* sp. (3%), *P. sordellii* (2%), and *P. bifermentans* (1%). Other species included *E. tarda* (1%), *C. ceti* (~1%), and *Ureaplasma* spp. (~1% combined). Viruses (0.6%) included Omikronpapillomavirus (13% of viruses),

identified as *Tursiops truncatus* papillomavirus 6, and also Lymphocystivirus (3% of viruses).

The **distal colon** had a relatively similar representation to the rectum, with Proteobacteria (34%) and Firmicutes (62%) dominating the sample (**Figure S10**). This sample was also overrepresented by *P. damsela* (27%) and had an even larger representation of Clostridia (61%), with *C. perfringens* the most abundant identified species (14%). *P. sordellii* (5%), *Romboutsia* sp. (3%), *P. bifermentans* (3%) were also present. Other species included *E. tarda* (3%), *Fusibacterium* spp. (1% combined) and *Ureaplasma* spp. (~1% combined).

The **proximal colon** was overly represented by Firmicutes of the Class Clostridia (81%), followed by Proteobacteria (8%) (**Figure S11**). Within Clostridia, the main species identified were *P. bifermentans* (7%), *P. sordellii* (6%), *Paraclostridium benzoelyticum* (3%), *C. perfringens* (2%) and *Romboutsia* sp. (2%), while outside the Firmicutes, *P. damsela* (3%) and bacterium 2013Arg42i (identified as *Candidatus Ichthyocystis hellenicum*) (5%) were also relatively common. Betaretroviruses were also represented (2%).

The **stomach** was overly represented by the bacterium 2013Arg42i (*Candidatus Ichthyocystis hellenicum*) (58%), followed by Tenericutes, especially *Ureaplasma* spp. (10% combined), and Proteobacteria, particularly *A. baumannii* (6%) (**Figure S12**). Eukaryotes made up 2% of this sample, with a few fungal species identified: *Rhunchosporium agropyri*, *Tortispora caseinolytica*, *Rhizopus delemar* and *Rhizophagus irregularis*. Among the viruses (0.7%), lymphocystivirus was observed (9% of viruses).

The **mouth** was comprised mainly of Proteobacteria (52%) and Bacteroidetes (31%), and to a much lesser extent Fusobacteria (5%), Tenericutes (4%) and Firmicutes (2%) (**Figure S13**). Among Proteobacteria, an unclassified Gammaproteobacteria bacterium was the most common (18%), followed by *Psychrobacter* (11%), while among Bacteroidetes, *Aureispira* sp. (27%), *Porphyromonas* spp. (18%) and *Tenacibaculum* spp. (18%) were largely represented. Among Tenericutes, *Mycoplasma* had a large representation (98%), with *M. elephantis* and other species identified. Among Fusobacteria, *O. salmonicida* was overrepresented (60%).

The **skin lesion 1** was overrepresented by Proteobacteria (89%), and to a much lesser extent by Bacteroidetes (9%) (**Figure S14**). *Vibrio* made up a large component of the sample overall (61%), and included several identified species, but particularly *V. harveyi* (7% of all bacteria). Another observed Proteobacteria was *Arcobacter* (3%), which was also represented by multiple species. An unclassified Gammaproteobacteria bacterium was also abundant (7%). Of the Bacteroidetes, *Tenacibaculum*, which was represented by various species, was the most abundant genus (5% of all bacteria).

The **skin lesion 2** had relatively similar composition to skin lesion 1, with mostly Proteobacteria (64%) and Bacteroidetes (21%), and *Vibrio* (45%), particularly *V. harveyi* (5%) (**Figure S15**). *Arcobacter* spp. (11% combined) and *Tenacibaculum* spp. (8% combined) were also present.

The **skin lesion 3** also showed mainly Proteobacteria (46%) and Bacteroidetes (48%) but had a greater diversity of representative genera (**Figure S16**). Apart from *Vibrio* (6%), *Arcobacter* (7%) and *Tenacibaculum* (13%) (*T. ovolyticum* with 8%), *Crocinitomix* spp. (7%)

and *Halocynthiibacter namhaensis* (4%) had relatively large representations. The unclassified Gammaproteobacteria bacterium was also abundant (5%).

The **skin lesion 4** was also mainly represented by Proteobacteria (52%) and Bacteroidetes (40%) (**Figure S17**). In this sample, *Aureispira* sp. (28%), *Vibrio* genomosp. (19%) and *Arcobater* spp. were the most common. The unclassified Gammaproteobacteria bacterium was also abundant (5%), followed by *Tenacibaculum* spp. (3% combined) and *Psychrobacter* spp. (3% combined).

The **non-lesioned skin** was dominated by Proteobacteria followed by Bacteroidetes, but differently from the lesioned skin, its most abundant genera were represented by *Alcanivorax* (24%), *Sphingopyxis* (11%), *Muricauda* (8%), *Pelagibacterium* (8%), and *Erythrobacter* (7%) (**Figure S18**).

The **seawater** was also mainly represented by Proteobacteria (67%) and Bacteroidetes (23%), with a few identified genera and species: *Glaciecola* sp., *Nereida ignava*, *Winogradskyella* sp., *Planktomarina temperata*, *Polaribacter* sp., *Polaribacter dokdonensis*, *Owenweeksia hongkongensis* (**Figure S19**). Viruses made up ~1% of this sample.

Other potential **pathogens** present in the dolphin *Hunter*, but at small numbers, included the bacteria *Erysipelothrix rhusiopathiae*, *Coxiella burnetii*, *Salmonella enterica*, *Staphylococcus aureus*, *Pasteurella multocida*, *Plesiomonas shigelloides*, *Legionella pneumophila* and *L. longbeachae*, *Arcanobacterium* spp., *Aeromonas* spp., *Actinomyces* spp., *Campylobacter* spp., *Helicobacter pylori* and *H. cetorum*, *Leptospira*, *Dermatophilus*, *Burkholderia*; and the fungi *Aspergillus oryzae*, *Candida* spp., and *Mucor*.

## Discussion

The metagenomic analysis successfully identified a range of microbial taxa present in the dolphin samples of the different body systems examined and in the sample of local seawater. The focus of the discussion here is on the microbes of pathogenic potential among the main taxa identified by the analysis.

### ***Urinary system: kidney***

The kidney had a unique overrepresentation of *H. penzbergensis*, followed by *Asinibacterium* sp. Both are part of the family Chitinophagaceae, which is a potential disease indicator of fish populations (Deng et al. 2021). *H. penzbergensis* was isolated from a purified water system (Eder et al. 2015), while *Asinibacterium* species can be associated with sites contaminated with hydrocarbons, heavy metals or radionucleotides (Brzoska et al. 2021).

### ***Sensory system***

*E. tarda* was the predominant taxon found in the ear. It is a facultatively anaerobic bacterium of the Hafniaceae family. The PM report indicated necrosuppurative otitis media and interna of this ear, and culture also indicated heavy growth of *E. tarda*. In fish, it causes edwardsiellosis. *E. tarda* has been reported in odontocetes, and has the potential to cause gastroenteritis, wound infections, and septicaemia, as suggested for a stranded sperm whale (Cools et al. 2013).

### ***Central nervous and Circulatory systems***

The brain was dominated by bacteria, with several *Corynebacterium* species, including *C. diphtheria*, *E. tarda*, and *C. perfringens*. *C. diphtheriae* is the main cause of diphtheria and is one of the most severe bacterial infections in humans. It typically affects the upper respiratory tract, but cutaneous (ulcer forming) and invasive infections, including of the heart, are also possible (Hadfield et al. 2000). *C. perfringens* is an anaerobic bacterium that can be found as a normal component of many environments, including the gastrointestinal tract of vertebrates, but it can cause enteritis by food poisoning, or gas gangrene when wounds become infected (Uzal et al. 2014).

Like the brain, the heart was mainly dominated by several species of *Corynebacterium*, and the Clostridia *C. perfringens*, and also *P. sordellii*, *P. bifermentans*, and *P. benzoelyticum*. *P. sordellii* is another bacterium associated with gas gangrene in humans and animals (Nyaoke et al. 2020).

Betaretroviruses also showed relatively large proportions in the brain and heart, and other of *Hunter*'s tissues. Endogenous retroviruses are common in vertebrate genomes and they are normally not associated with disease (Baillie et al. 2004). Betaretroviruses were mainly represented in the dolphin tissue samples, but not the swabs, likely due to the difficulty of fully filtering out the host genome from sequences originated from tissue-extracted DNA.

### ***Digestive system: mouth, stomach, colon, rectum, and liver***

The mouth was represented by diverse bacteria, including *Psychrobacter*, *Aureispira* sp., *Porphyromonas* spp., *Tenacibaculum* spp., *Mycoplasma* spp. and *O. salmonicida*. *Psychrobacter* can cause human infections such as endocarditis and peritonitis, but has been found in abundance in the skin of managed killer whales and bottlenose dolphins (Chiarello et al. 2017). *Aureispira* is part of the Saprospiraceae, which mainly inhabit aquatic environments and activated sludge, and breakdown complex organic compounds (McIlroy

and Nielsen 2014). *Porphyromonas* are obligatory anaerobic bacteria which are part of the salivary microbiome. The most studied, *P. gingivalis*, is considered an important pathogen associated with human periodontal disease (How et al. 2016). *Porphyromonas* are known to be present in the oral cavity of many cetaceans, and may be part of its core microbial community but increase in abundance in animals with a diseased status (Soares-Castro et al. 2019). *Tenacibaculum* spp. are associated with disease in fish and molluscs, called tenacibaculosis, which can cause epidermal ulcers, atypical behaviors, and mortality, and are of major concern in mariculture (Nowlan et al. 2020). *O. salmonicida* is a known pathogen of fish and can lead to high mortalities, but many marine mammal species seem to act as their hosts (Glaeser and Semmler 2020). Several species of *Mycoplasma* are pathogenic to humans and also marine mammals, and they involved in respiratory and inflammatory diseases (Waltzek et al. 2012). Post-mortem culture of a mouth swab of *Hunter* suggested moderate growth of the bacterium *Vibrio anguillarum*, but *Vibrio* spp. was only 1% of the bacteria identified by metagenomics. Lymphocystis virus was also observed by the metagenomics analysis in several *Hunter* samples, but mainly in the mouth and stomach. Lymphocystis is a common viral disease of fish (Borrego et al. 2015), and could have been associated with the dolphin prey.

The (pyloric) stomach was dominated by bacterium 2013Arg42i, which has been named *Candidatus Ichthyocystis hellenicum*. Other abundant species present included *Ureaplasma* spp. and *A. baumannii*. The PM report indicated haemorrhagic gastritis of this section of the stomach. *Candidatus Ichthyocystis hellenicum* is an emerging pathogen isolated from seabream that causes epitheliocystis in fish (Seth-Smith et al. 2016). *A. baumannii* can cause infections of the skin, bloodstream, urinary tract, and other soft tissues. It can be an opportunistic pathogen in humans, affecting mainly people with compromised immune systems. *Ureaplasma* spp. have been reported in the stomach of both sick and apparently healthy wild dolphins (Bik et al. 2016, Gody-Vitorino et al. 2017).

The proximal colon was mainly represented by Clostridia species such as *P. sordelii*, *P. benzoelyticum* and *P. bifermentans*, but also *Candidatus Ichthyocystis hellenicum*. *P. bifermentans* and *P. benzoelyticum* are found in many environments, including polluted waters, and can be isolated from wounds, blood, and ulcers. The distal colon was overrepresented by *P. damsela*, but also the main Clostridia species observed in the distal colon and *C. perfringens*. *P. damsela* is a pathogen of a variety of marine animals including fish, crustaceans, molluscs, and cetaceans (Rivas et al. 2013). The geographical distribution of this bacterium is increasing, and it is an emerging pathogen of fish farms. It can also be pathogenic for humans and cause septicaemia or infection to wounds (Rivas et al. 2013). *Photobacterium* was reported as abundant in the colon of an edematous female striped dolphin stranded in Portugal (Gody-Vitorino et al. 2017), and in wounds of bottlenose dolphins (Fujioka et al. 1988). *C. perfringens* was reported as abundant in the distal colon of live bottlenose dolphins (Robles-Malagamba et al. 2020), and involved in septicemia in a stranded common dolphin (Danil et al. 2014) and necrotising enteritis in captive bottlenose dolphins (Salbany et al. 2011). Like the distal colon, the rectum showed an abundance of *P. damsela* and Clostridia, but particularly *C. perfringens*. *Hunter*'s PM report indicated haemorrhagic gastritis and enteropathy, with *C. perfringens* growth in cultures from the stomach, distal intestine and faeces, and *P. damsela* and *E. tarda* in the distal intestine and faeces. *Cetobacterium* spp., which have been reported as highly abundant in the distal colon of healthy free-ranging and captive bottlenose dolphins in the northern hemisphere (Bik et al. 2006, Robles-Malagamba et al. 2020), had a low representation in the ADS dolphin. The rectum also included a relative proportion of Omikronpapillomavirus, represented by *T.*

*truncatus* papillomavirus 6. In dolphins, they are associated with a high prevalence of orogenital tumours (Rodriguez et al. 2018).

The liver sample had relatively large representations of *C. perfringens* and *C. abortus*. Other species present were *C. ceti* and *C. diphtheria*. *C. abortus* is a species that causes abortion and foetal death in mammals, including humans, and is transmitted orally and sexually among mammals (Longbottom and Coulter 2003). *C. abortus* has been recently isolated, and identified as likely causing the death of a striped dolphin from Italy that died with liver congestion, splenic lymphoid, and pneumonia (Santoro et al. 2019). *C. ceti* has been reported as part of the intestinal microbiota of several odontocetes, including bottlenose dolphins (e.g., Bik et al. 2016).

#### ***Lymphatic system: spleen***

The spleen also showed various bacterial species, with mention to *N. polysaccharea*, *M. tuberculosis*, and *A. naeslundii*. *M. tuberculosis* is a pathogenic bacterium that causes tuberculosis, but there is recent evidence from humans of association with multiple other diseases (Chai et al. 2018). Tuberculosis caused by *M. pinnipedii* has been diagnosed in New Zealand pinnipeds and one cetacean, with ingestion in the latter identified as the possible route (Roe et al. 2019). *A. naeslundii* is generally found in the mouth of humans and has been associated to periodontal disease (Li et al. 2018).

#### ***Respiratory system: blowhole and lung***

The blowhole was represented by various taxa, but *Tenacibaculum* and *Chryseobacterium* were the most abundant. One species, *O. rhinotracheale*, was characteristic of this sample. *Tenacibaculum* was isolated from the blowhole of a stranded striped dolphin, and apparently healthy wild bottlenose dolphins (Gody-Vitorino et al. 2017, Robles-Malagamba et al. 2020). *Chryseobacterium* contains over 100 described species and are found in various habitats, including freshwater, soil, marine fish, and humans (Mwanza et al. 2022). Some of the species can cause disease, such as bacteremia, peritonitis, pneumonia, among others. Members of this genus have been isolated from the blow of bottlenose dolphins at Shark Bay (Nelson et al. 2019). *O. rhinotracheale*, causes respiratory disease in poultry, but it is not currently considered a zoonosis (Barbosa et al. 2020). From culture done as part of the post-mortem investigation, *Vibrio* and *Salinivibrio* showed a moderate growth, but they made up less than 1% of the taxa identified by the metagenomics analysis.

The lung also showed a variety of species present, and particularly *C. diphtheriae*, *C. jejuni*, *B. cereus*, and *N. polysaccharea*. *C. jejuni* is one of the most common causes of gastroenteritis in the world, and is normally associated with poultry, and found in animal faeces (Galanis 2007). *B. cereus* is a bacterium that produces toxins that cause vomiting and diarrhoea (Granun and Lund 1997). *N. polysaccharea* is not considered a pathogenic bacterium (Clemence et al. 2018).

#### ***Integumentary system: lesioned and non-lesioned skin***

The PM report indicated the presence of multiple cutaneous abscesses in the dolphin *Hunter*, some of which were swabbed for this study, including the two major skin lesions observed in the animal (skin lesions 1 and 2). The lesioned skin was mainly composed of *V. harveyi*, *V. genomosp.*, *Arcobacter*, *Aureispira* sp., and *T. ovolyticum*. *V. harveyi* is a bioluminescent bacterium which is considered a major pathogen of marine fish and invertebrates, especially penaeid shrimp (Zhang et al. 2020). Diseased fish may exhibit a range of lesions, including eye lesions, gastroenteritis, muscle necrosis, and skin ulcers, and it can also be identified as

part of a mixed *Vibrio* community in diseased animals (Zhang et al. 2020). *V. harveyi* was also identified through culture methods as part of the post-mortem investigation of *Hunter*. *Arcobacter* can be found in a range of habitats, and some species can be pathogens to humans and animals (Ramees et al. 2016). Species of the genus may cause bacteremia, endocarditis, peritonitis, gastroenteritis and diarrhea (Ramees et al. 2016). This genus has been reported in various body regions of bottlenose dolphins (Robles-Malagamba et al. 2020).

The non-lesioned had a very different main microbial composition to the lesioned skin. The non-lesioned skin was characterised by several genera, such as *Alcanivorax*, *Sphingopyxis*, *Muricauda*, *Pelagibacterium*, and *Erythrobacter*. *Alcanivorax* are characteristic of oil-contaminated waters where nitrogen and phosphorus are not limiting and can play a role in the biological clean-up of oil-contaminated environments (Schneiker et al. 2006). *Sphingopyxis* species have the potential to degrade several xenobiotics and other environmental contaminants that impose a threat to human health (Sharma et al. 2020). The presence of these genera in *Hunter*'s normal skin suggests the presence of point sources of pollution within the dolphin's range (e.g. Russo et al. 2018).

Differences in the diversity and abundance of microbial taxa in the different body organs of the ADS dolphin corroborates the idea that distinct physiochemical conditions influence their microbiomes (Robles-Malagamba et al. 2020), but can also be affected by its disease status.

### ***Seawater around Garden Island***

The seawater composition was very different to the dolphin samples. It had a great diversity of taxa, but few could be identified at the species level, such as *N. ignava*, *P. temperata*, *P. dokdonensis*, and *O. hongkongensis*. These species do not appear to be associated with disease status in marine vertebrates.

The study focused here on bacteria, viruses, Archaea and fungi identified in the samples of ADS dolphin *Hunter* and the seawater around Garden Island on the day of the animal's death. However, the gene catalogue from the metagenomic analysis of *Hunter* is available to further explore the presence of other microbial (algae, protozoa) and non-microbial eukaryotes (fish and invertebrates in the gut) and for a comparison to the current results. Given the identification of several known fish and to a lesser extent invertebrate pathogens in the dolphin samples, it would be worth considering additional studies looking at the microbial composition of the dolphin prey in the ADS. In addition, characterising spatial and temporal variation in the seawater microbial community of the Port River system, especially around wastewater outflows, would be valuable to understand potential risks to dolphins, other wildlife, and the public.

## Conclusions

This metagenomic study provides the first comprehensive inventory of microorganisms in an diseased ADS dolphin. It showed major differences in the diversity and abundance of microbial taxa in the different body systems and organs examined, including in lesioned vs non-lesioned skin, as well as in the local seawater. Several microorganisms of pathogenic potential, many of which were not previously known for this dolphin population, were identified in *Hunter*, including various zoonotic agents. In addition, bacteria associated with polluted environments were observed in the dolphin's non-lesioned skin. The study demonstrates the feasibility and value of using shotgun metagenomics for microbial and pathogen surveillance in ADS dolphins and its environment. The information provided here is relevant for future health studies of these dolphins and the Port River system, management of ill animals, and for potentially mitigating risks to wildlife and human health.

## Acknowledgments

Permission to collect samples from dolphin *Hunter* was given by DEW, and assistance on site by its staff, especially Jon Emmett, Verity Gibbs, Darryl Cowan and Chloe McSkimming, and by ZooSA's veterinarian, Dr Ian Smith. Assistance to collect samples during post-mortem examination at the Veterinary Diagnostic Laboratory was given by A/Prof Lucy Woolford, Dr Ikuko Tomo, Dr Anne-Lise Chaber, Dr Rebecca Souter, Dr Mike Bossley, and Adrian Hines. Assistance at the Molecular Ecology Laboratory, Flinders University, was provided by Diana-Elena Vornicu and Gabrielle Genty. Sequencing and initial bioinformatics was conducted at Novogene. Advice about the metagenomic analysis was given by Prof Elizabeth Dinsdale and Dr Michael Roache from Flinders Accelerator for Microbiome Exploration, and A/Prof Sophie Leterme. Funding for the metagenomic analysis was provided by DEW and Flinders University. This study is a contribution to the ADS Investigation led by Dr Lisien Loan, Director of Conservation and Wildlife Management, DEW.

## References

- Baillie et al. 2004. Multiple Groups of Endogenous Betaretroviruses in Mice, Rats, and Other Mammals. *J. Virol.* 78, 5784.
- Barbosa et al. 2020. *Ornithobacterium rhinotracheale*: An Update Review about An Emerging Poultry Pathogen. *Vet. Sci.* 7, 3.
- Bik et al. 2016. Marine mammals harbor unique microbiotas shaped by and yet distinct from the sea. *Nat. Commun.* 7, 10516.
- Borrego et al. 2015. Lymphocystis disease virus: its importance in aquaculture. *Rev. Aquacult.* 9, 179.
- Bossart GD (2011) Marine mammals as sentinel species for oceans and human health. *Veterinary Pathology* 48, 676-690.
- Bossley M, Steiner A, et al. (2007) A long-term study of bottlenose dolphins (*Tursiops aduncus*) in an Australian industrial estuary: increased sightings associated with environmental improvements. *Marine Mammal Science* 33, 241-251.
- Brzoska et al. 2021. Physiological and Genomic Characterization of Two Novel Bacteroidota Strains *Asinibacterium* spp. OR43 and OR53. *Bact.* 1, 33–47.
- Buchfink et al. 2014. Fast and Sensitive Protein Alignment Using DIAMOND. *Nat. Meth.*, 12, 59.
- Byard RW, Machado A et al. (2020) Lethal fishing penetration and line entanglement in an adult bottlenose dolphin (*Tursiops aduncus*). *Forensic Science, Medicine and Pathology* 16, 540-543.
- Chai et al. 2018. *Mycobacterium tuberculosis*: an adaptable pathogen associated with multiple human diseases. *Front. Cell Infect. Microbiol.* 8, 158.
- Chiarello et al. 2017. Captive bottlenose dolphins and killer whales harbour a species-specific skin microbiota that varies among individuals. *Sci. Rep.* 7, 15269.
- Clemence et al. 2018. Characterization of capsule genes in non-pathogenic *Neisseria* species. *Microb. Genom.* 4, e000208.
- Cools et al. 2013. *Edwardsiella tarda* sepsis in a live-stranded sperm whale (*Physeter macrocephalus*). *Vet. Microb.* 166, 311.
- Currie JJ, van Aswegen et al. (2021) Rapid weight loss in free ranging pygmy killer whales (*Feresa attenuata*) and the implications for anthropogenic disturbance of odontocetes. *Scientific Reports* 11, 1.
- Danil et al. 2014. *Clostridium perfringens* septicemia in a long-beaked common dolphin *Delphinus capensis*: an etiology of gas bubble accumulation in cetaceans. *Dis. Aquat. Org.* 111, 183.
- Department of Environment and Heritage (2008). Adelaide Dolphin Sanctuary Management Plan 25pp.
- Deng et al. 2021. Shifts in pond water bacterial communities are associated with the health status of sea bass (*Lateolabrax maculatus*). *Ecol. Indic.* 127, 107775
- Eder et al. 2015. *Hydrobacter penzbergensis* gen. nov., sp. nov., isolated from purified water. *Int. J. Syst. Evol. Microbiol.* 65.

- Environment Protection Authority (2003) Water Quality of the Port River Estuary – community summary. EPA Report 6pp.
- Environment Protection Authority (2005) Setting Environmental Values for the Port Waterways. EPA Report 29pp.
- Fire SE, Wanj ZH et al. (2011) Co-occurrence of multiple classes of harmful algal toxins in bottlenose dolphins (*Tursiops truncatus*) stranding during an unusual mortality event in Texas, USA. Harmful algae 10, 330-336.
- Fujioka et al. 1988. *Vibrio damsela* from wounds in bottlenose dolphins *Tursiops truncatus*. Dis. Aquat. Org. 4, 1.
- Galanis 2007. *Campylobacter* and bacterial gastroenteritis. CMAJ 177, 570.
- Glaeser and Semmler 2020. Marine mammals are natural hosts of *Oceanivirga salmonicida*, a bacterial pathogen of Atlantic salmon. Dis. Aquat. Org. 139, 161.
- Godoy-Vitorino et al. 2017. The microbiome of a striped dolphin (*Stenella coeruleoalba*) stranded in Portugal. Res Microbiol. 168, 85.
- Granun and Lund 1997. *Bacillus cereus* and its food poisoning toxins. FEMS Microbiol. Lett. 157, 223.
- Hadfield et al. 2000. The pathology of diphtheria. J. Infect. Dis. 181, S116.
- How et al. 2016. *Porphyromonas gingivalis*: an overview of periodontopathic pathogen below the gum line. Front. Microbiol. 7, 53.
- Langmead and Salzberg 2012. Fast gapped-read alignment with Bowtie 2. Nat. Meth. 9, 357.
- Li et al. 2014. An integrated catalog of reference genes in the human gut microbiome. Nat. Biotechnol. 32, 834.
- Li et al. 2018. *Actinomyces* and alimentary tract diseases: a review of its biological functions and pathology. Biomed. Res. Int. 2018, 3820215.
- Longbottom and Coulter 2003. Animal chlamydiosis and zoonotic implications. J. Comp. Pathol. 128, 217.
- Mwanza et al. 2022. Pathogenic Potential and Control of *Chryseobacterium* Species from Clinical, Fish, Food and Environmental Sources. Microorganisms 10, 895.
- McIlroy and Nielsen 2014. The Family *Saprospiraceae* in *The Prokaryotes* (Eds Rosunberg et al.). Springer. p. 863.
- Mende et al. 2012. Assessment of Metagenomic Assembly Using Simulated Next Generation Sequencing Data. PLoS One 7, e31386.
- Nelson et al. 2019. Detecting respiratory bacterial communities of wild dolphins: implications for animal health. MEPS 622, 203.
- Nielsen et al. 2014. Identification and assembly of genomes and genetic elements in complex metagenomic samples without using reference genomes. Nat. Biotechnol. 32, 822.

- Nowlan et al. 2020. Advancements in Characterizing *Tenacibaculum* Infections in Canada. *Path.* 9, 1029.
- Nyaoke et al. 2020. Paeniclostridium (Clostridium) sordellii-associated enterocolitis in 7 horses. *J. Vet. Diagn. Invest.* 32, 239.
- Ondov et al. 2011. Interactive metagenomic visualization in a web browser. *BMC Bioinformatics* 1.
- Palmer et al. 2020. Marine mammals are natural hosts of *Oceanivirga salmonicida*, a bacterial pathogen of Atlantic salmon. *Dis. Aquat. Organ.* 139, 161.
- Ramees et al. 2016. *Arcobacter*: an emerging food-borne zoonotic pathogen, its public health concerns and advances in diagnosis and control – a comprehensive review. *Vet. Quart.* 37.
- Rivas et al. 2013. *Photobacterium damsela* subsp. *damsela*, a bacterium pathogenic for marine animals and humans. *Front. Microbiol.* 4, 283.
- Rodriguez et al. 2018. Complete Genome Sequencing of a Novel Type of *Omikronpapillomavirus 1* in Indian River Lagoon Bottlenose Dolphins (*Tursiops truncatus*). *Genome Announc.* 6, e00240-8.
- Roe et al. 2019. Pathology and molecular epidemiology of *Mycobacterium pinnipedii* tuberculosis in native New Zealand marine mammals. *PLoS One* 14, e0212363.
- Russo et al. 2018. Bacterial species identified on the skin of bottlenose dolphins off Southern California via Next Generation Sequencing Techniques. *Microbiol. Aquat. Syst.* 75, 303.
- Salbany et al. 2011. *Clostridium perfringens* Alpha Toxin Infection in a Group of Indo-Pacific Bottlenose Dolphins (*Tursiops aduncus*) in the United Arab Emirates (UAE). International Association for Aquatic Animal Medicine, Conference Proceedings.
- Santoro et al. 2019. Molecular detection of *Chlamydia abortus* in a stranded Mediterranean striped dolphin *Stenella coeruleoalba*. *Dis. Aquat. Organ.* 132, 203.
- Schneiker et al. 2006. Genome sequence of the ubiquitous hydrocarbon-degrading marine bacterium *Alcanivorax borkumensis*. *Nat. Biotech.* 25, 997.
- Sharma et al. 2020. The genus *Sphingopyxis*: systematics, ecology, and bioremediation potential - a review. *J. Environ. Manage.* 280:111744
- Seth-Smith et al. 2016. Emerging pathogens of gilthead seabream: characterisation and genomic analysis of novel intracellular  $\beta$ -proteobacteria. *ISME J.* 10, 1791.
- Soares-Castro et al. 2019. Microbial fingerprints within the oral cavity of cetaceans as indicators for population monitoring. *Sci. Rep.* 9, 13679.
- Uzal et al. 2014. Towards an understanding of the role of *Clostridium perfringens* toxins in human and animal disease. *Future Microbiol.* 9, 361.
- Van Bresse MF, Raga JA et al. (2009) Emerging infectious diseases in cetaceans worldwide and the possible role of environmental stressors. *Disease of Aquatic Organisms* 86, 143-157.

Waltzek et al. 2012. Marine Mammal Zoonoses: A Review of Disease Manifestations. Zoon. Publ. Health 59, 521.

Wang XY, Wu FX et al. (2017) Long-term changes in the distribution and core habitat use of a coastal delphinid in response to anthropogenic coastal alterations. Aquatic Conservation-Marine and Freshwater Ecosystems 27, 643-652.

Wells R, Rhinehart H, Hansen L, et al. (2004) Bottlenose Dolphins as Marine Ecosystem Sentinels: Developing a Health Monitoring System. EcoHealth 1.

Zhang et al. 2020. *Vibrio harveyi*: a serious pathogen of fish and invertebrates in mariculture. Mar. Life Sci. & Techn. 2, 231.

Zeller et al. 2014. Potential of faecal microbiota for early-stage detection of colorectal cancer. Mol. Syst. Biol. 10, 766.

**Table S1.** Details of samples collected from the ADS dolphin *Hunter* on 22/10/21, and of water samples.

Sample	Abbreviation	Body system	Sample type	Time since death	DNA quantity (ng)	Sequenced Novogene
Brain	HBR	Central nervous	Tissue	≤ 3 hrs	10.8	Y
Heart	HHE	Circulatory	Tissue	≤ 3 hrs	12.7	Y
Mouth (tongue)	HMT	Digestive	Swab	≤ 20 min	35.6	Y
Stomach (pyloric)	HST	Digestive	Swab	≤ 3 hrs	8.9	Y
Colon (Proximal)	HCO2	Digestive	Swab	≤ 3 hrs	112	Y
Colon (Distal)	HCO1	Digestive	Swab	≤ 3 hrs	173	Y
Rectum	HRE	Digestive	Swab	≤ 20 min	23.6	Y
Genital Slit	HE	Reproductive	Swab	≤ 20 min	2.2	N
Liver	HLI2	Digestive	Tissue	≤ 3 hrs	140	Y
Spleen	HSP	Lymphatic	Tissue	≤ 3 hrs	26	Y
Blow	*	Respiratory	Swab	≤ 20 min	1.93	N
Blowhole	HBL	Respiratory	Swab	≤ 20 min	14.1	Y
Lung	HLU	Respiratory	Tissue	≤ 3 hrs	31.6	Y
Ear (left)	HEA	Sensory	Swab	≤ 3 hrs	140	Y
Eye (right)	*	Sensory	Swab	≤ 20 min	2.2	N
Eye (left)	*	Sensory	Swab	≤ 20 min	3.19	N
Kidney	HKI	Urinary	Tissue	≤ 3 hrs	45.6	Y
Skin Lesion 1	HSL1	Integumentary	Swab	≤ 20 min	330	Y
Skin Lesion 2	HSL2	Integumentary	Swab	≤ 20 min	24	Y
Skin Lesion 3	HSL3	Integumentary	Swab	≤ 20 min	17.6	Y
Skin Lesion 4	HSL4	Integumentary	Swab	≤ 20 min	53.5	Y
Non-lesion skin (clean)	HSC	Integumentary	Swab	≤ 20 min	10.5	Y
Water Garden Island 22/10/21	HWGI	NA	Water	NA	75.5	Y
Water Garden Island 26/11/21	*	NA	Water	NA	3.6	N
Water Snowden Beach 26/11/21	*	NA	Water	NA	3.67	N

**Table S2.** Results of data quality control applied to the raw data post-sequencing of dolphin and seawater samples by Novogene.

#Sample	InsertSize (bp)	RawData	CleanData	Clean_Q20	Clean_Q30	Clean_GC (%)	Effective (%)
HBL	350	12,530.70	12,514.83	97.51	92.44	36.64	99.873
HLU	350	12,252.91	12,202.41	96.89	92.13	41.56	99.588
HEA	350	12,416.74	12,341.90	96.33	91	42.14	99.397
HSL2	350	12,200.27	12,146.57	96.63	91.57	42.02	99.56
HRE	350	12,278.04	12,174.00	97	92.44	41.74	99.153
HSP	350	12,021.47	11,951.47	96.82	92.11	41.8	99.418
HBR	350	12,905.56	12,856.23	97.02	92.44	43.44	99.618
HKI	350	12,221.02	12,181.05	96.54	91.3	41.12	99.673
HCO2	350	12,032.76	11,978.78	96.69	91.72	41.56	99.551
HSL4	350	12,216.10	12,111.51	96.69	91.86	43.18	99.144
HSC	350	13,128.42	13,095.86	98.31	94.84	59.51	99.752
HST	350	12,146.16	11,965.82	96.62	92.18	44.18	98.515
HSL3	350	12,290.03	12,249.70	97.48	92.64	39.8	99.672
HMT	350	12,415.87	12,341.29	96.5	90.66	41.91	99.399
HLI	350	12,356.05	12,284.37	97.33	92.53	41.4	99.42
HHE	350	12,590.91	12,542.31	97.28	92.5	41.29	99.614
HSL1	350	12,089.74	11,996.19	96.62	91.52	44.65	99.226
HWGI	350	12,468.42	12,447.95	97.25	92.45	45.14	99.836
HCO1	350	12,176.32	12,083.00	96.62	91.55	44.1	99.234

**Notes:** **Clean\_Q20** is the percentage of bases whose quality score is greater than 20 or error rate is less than 0.01; **Clean\_Q30** is the percentage of bases whose quality score is greater than 30 or error rate is less than 0.001; **Effective** is the ratio of the CleanData over the RawData.

**Table S3.** Results of the metagenome assembly of dolphin and seawater samples by Novogene.

SampleID	Total len. (bp)	Num.	Average len. (bp)	N50 Len. (bp)	N90 Len. (bp)	Max len. (bp)
HBL	208,262,481	158,404	1,314.76	1,560	603	159,284
HLU	1,067,898	1,379	774.4	742	534	11,808
HEA	1,248,071	1,627	767.1	723	530	6,836
HSL2	1,100,377	1,450	758.88	715	529	8,020
HRE	31,863,869	20,330	1,567.33	2,313	615	242,143
HSP	995,155	1,291	770.84	728	531	6,307
HBR	1,418,550	1,780	796.94	790	541	6,334
HKI	4,577,130	1,091	4,195.35	162,473	771	487,355
HCO2	959,587	1,256	764	719	531	8,038
HSL4	17,093,293	13,633	1,253.82	1,397	587	134,853
HSC	214,172,768	120,074	1,783.67	2,827	657	594,103
HST	57,930,073	84,624	684.56	634	518	212,318
HSL3	135,694,107	59,584	2,277.36	5,822	733	1,017,651
HMT	49,841,411	32,159	1,549.84	2,228	616	117,167
HLI	939,478	1,231	763.18	719	527	11,301
HHE	997,540	1,276	781.77	740	529	10,150
HSL1	13,371,708	6,285	2,127.56	4,482	721	128,996
HWGI	229,452,496	197,438	1,162.15	1,274	586	334,448
HCO1	14,965,220	7,552	1,981.62	5,296	661	571,411
NOVO_MIX	9,915,604	14,648	676.93	655	522	2,807

**Notes:** **SampleID** is the name of the samples; **Total Len. (bp)** is the length of all the Scaffigs; **Num.** is the total number of Scaffigs; **Average Len. (bp)** is the average length of all the Scaffigs; **N50 Len.(bp)** is the shortest sequence length at 50% of the genome; **N90 Len.(bp)** is the shortest sequence length at 90% of the genome; **Max Len** is the max length of the Scaffigs.

**Table S4.** Gene catalogue statistics of dolphin and seawater samples by Novogene.

<b>ORFs NO.</b>	<b>1,168,229</b>
integrity: all	512,971 (43.91%)
integrity: end	251,123 (21.5%)
integrity: start	298,211 (25.53%)
integrity: none	105,924 (9.07%)
Total Len. (Mbp)	748.66
Average Len. (bp)	640.85
GC percent	45.83

**Notes:** **ORFs NO.** is the number of genes in gene catalogue; **integrity: start** is the amount and percentage of genes only containing start codons; **integrity: end** is the amount and percentage of genes only containing stop codons; **integrity: none** is the amount and percentage of genes not containing start or stop codons; **integrity: all** is the amount and percentage of genes containing both start and stop codons; **Total Len. (Mbp)** is the total length of the gene catalogue (millions); **Average Len.** is the average length of genes in the gene catalogue; **GC Percent** is the prediction of GC content of genes in the gene catalogue.

**Figure S1.** Krona chart depicting relative abundance of taxonomic groups at different hierarchical levels in the kidney sample.

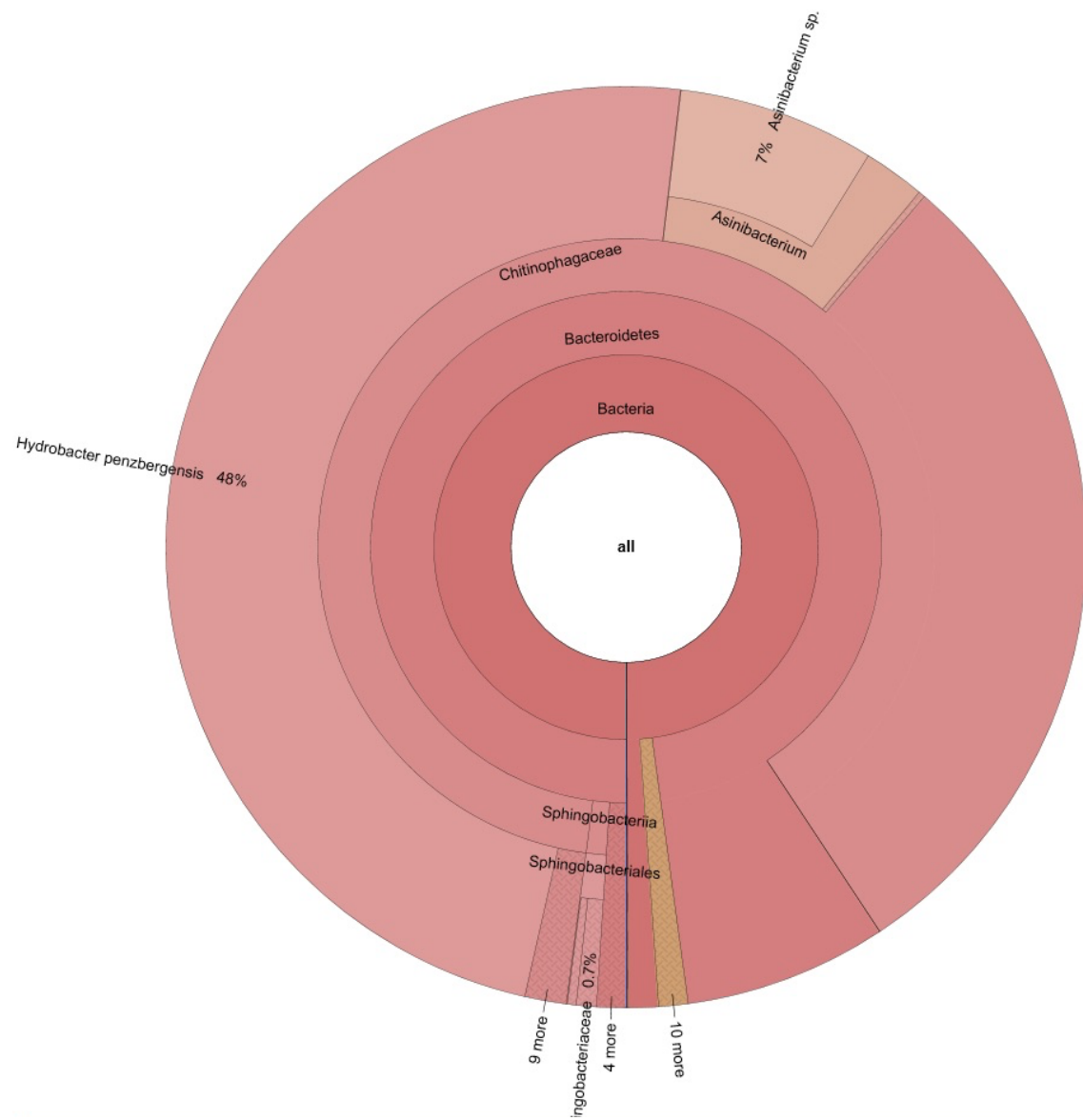


**Figure S2.** Krona chart depicting relative abundance of taxonomic groups at different hierarchical levels in the ear sample.

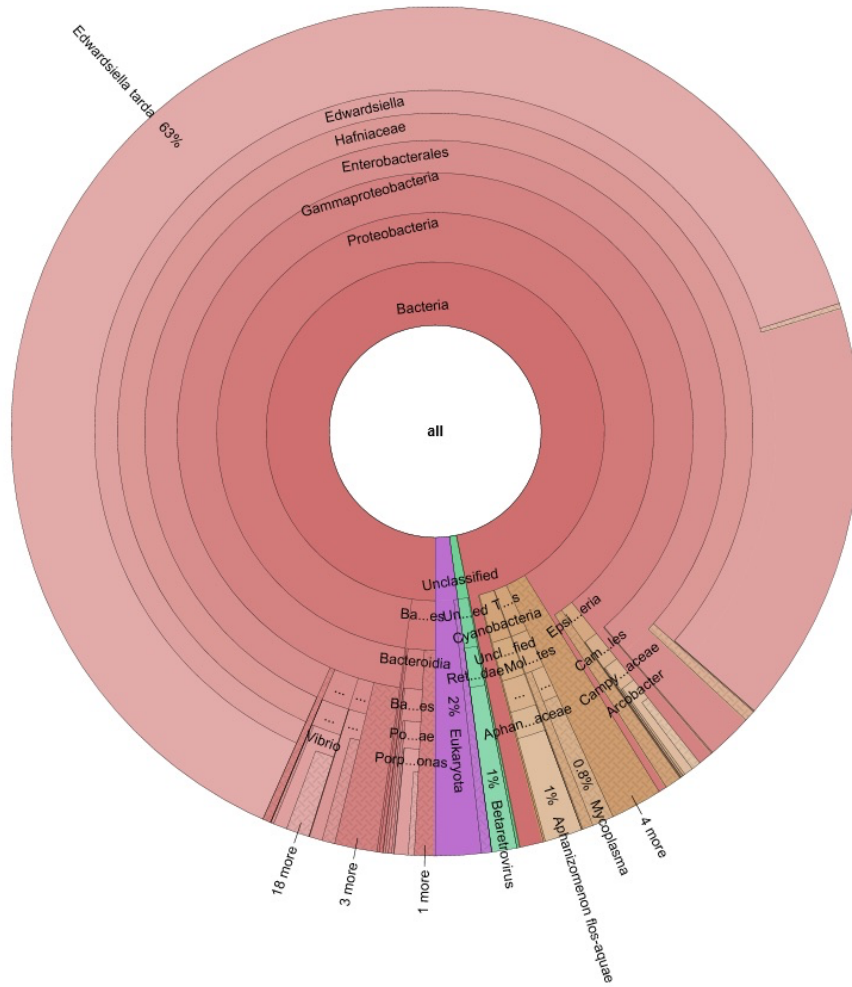






**Figure S5.** Krona chart depicting relative abundance of taxonomic groups at different hierarchical levels in the liver sample.

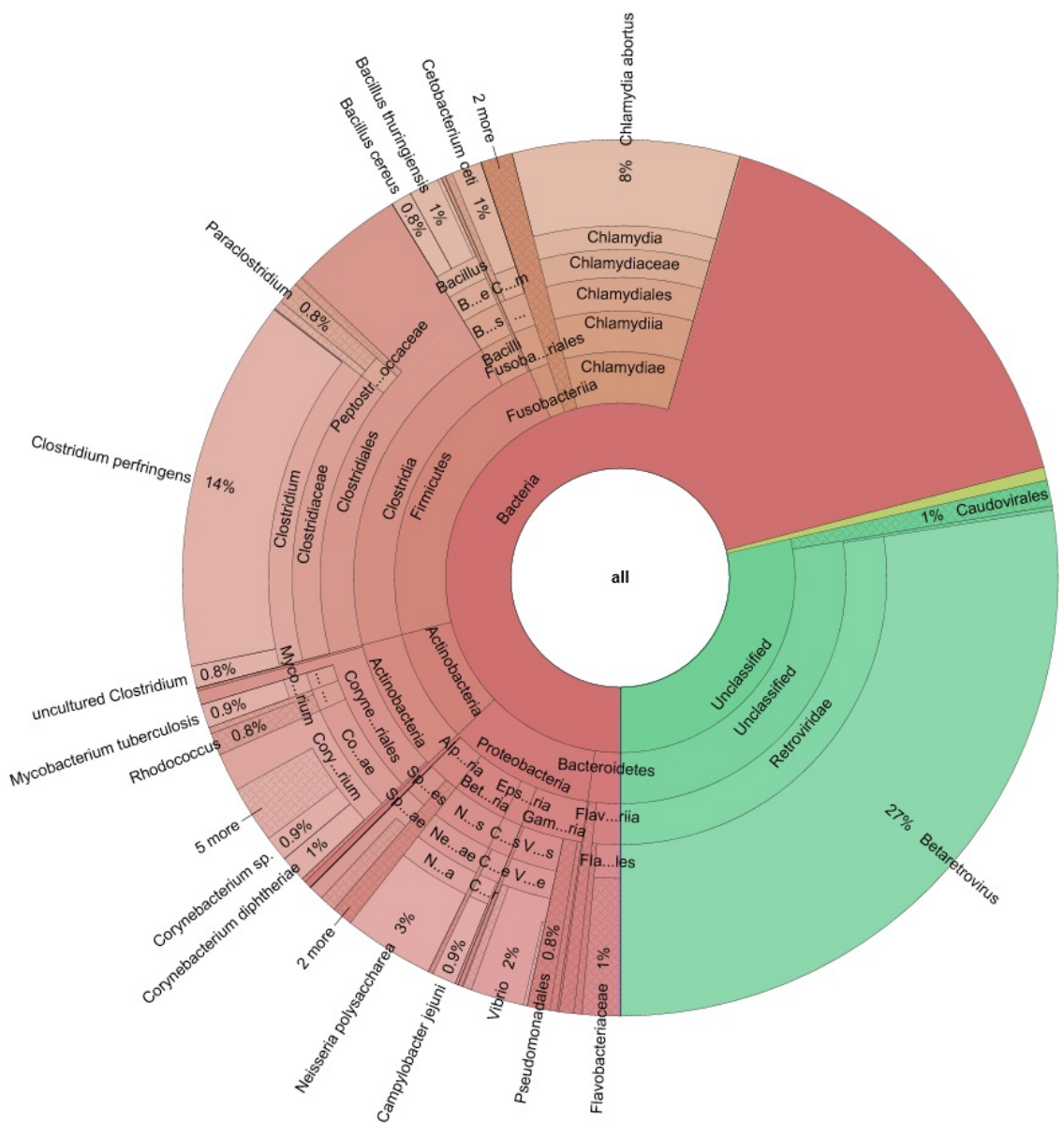


**Figure S6.** Krona chart depicting relative abundance of taxonomic groups at different hierarchical levels in the spleen sample.

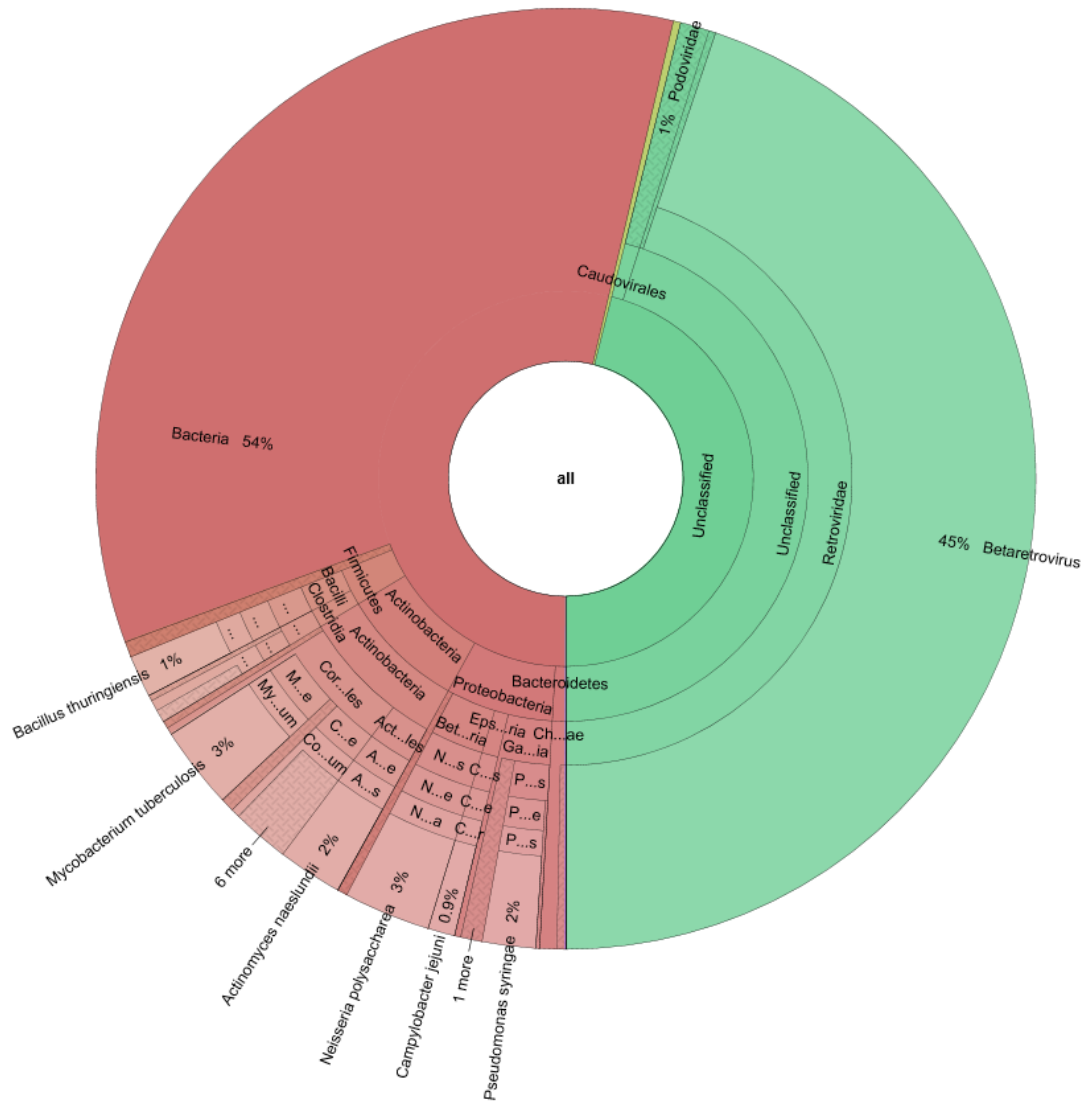




**Figure S8.** Krona chart depicting relative abundance of taxonomic groups at different hierarchical levels in the blowhole sample.

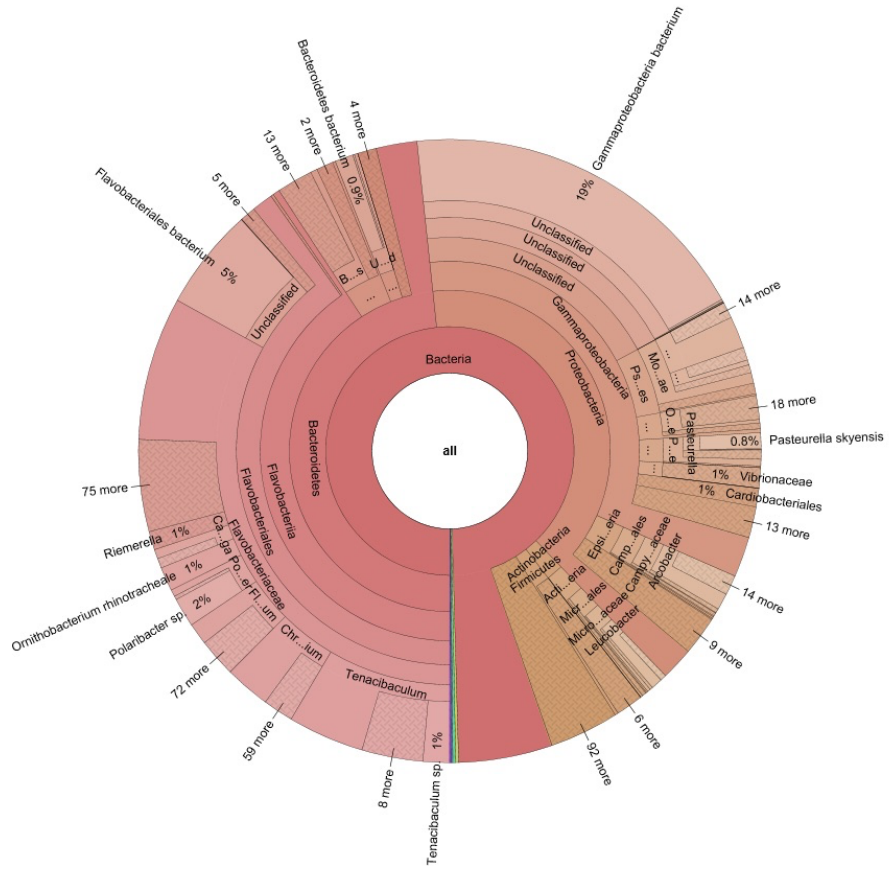


**Figure S9.** Krona chart depicting relative abundance of taxonomic groups at different hierarchical levels in the rectum sample.

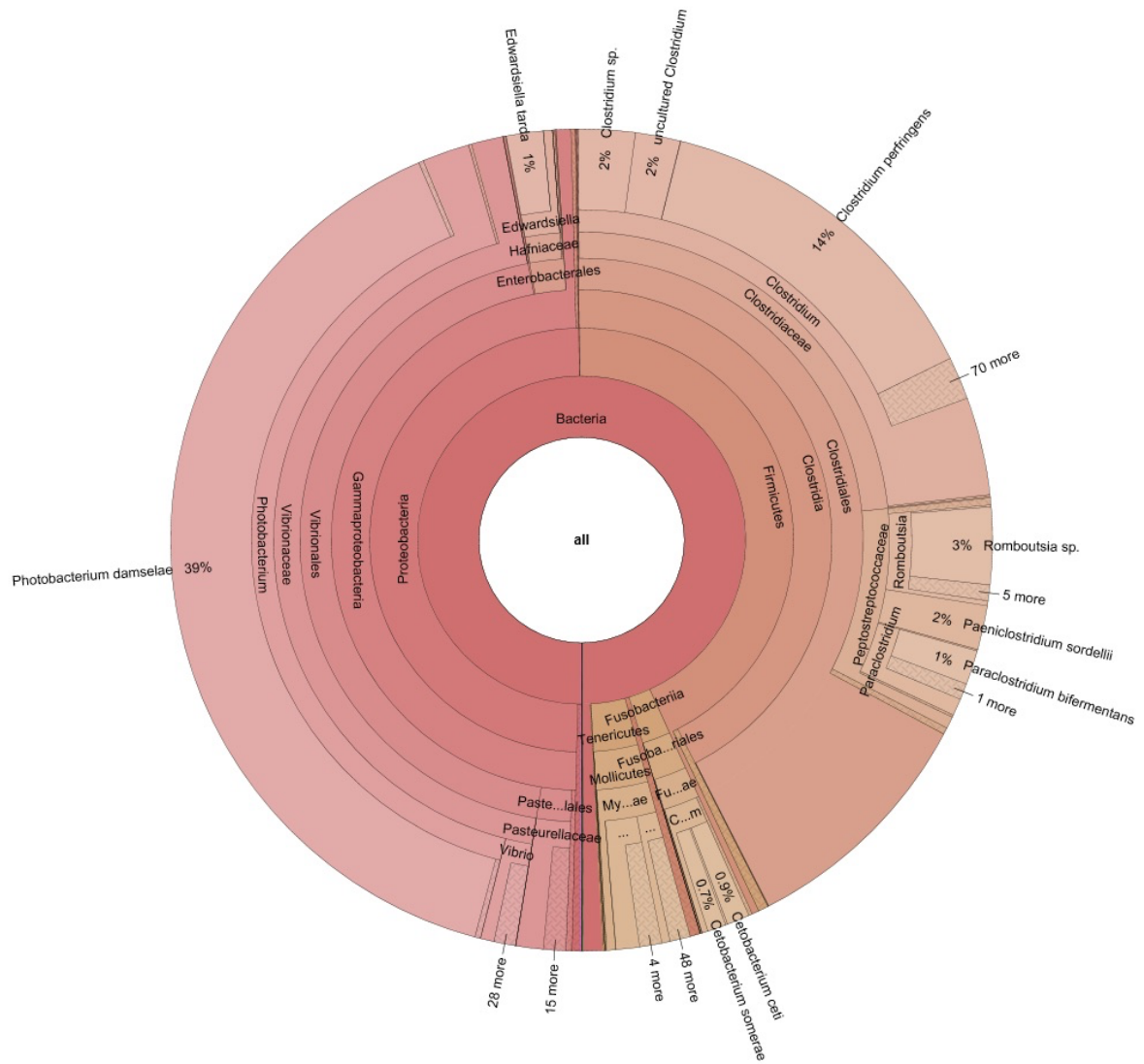


**Figure S10.** Krona chart depicting relative abundance of taxonomic groups at different hierarchical levels in the distal colon sample.

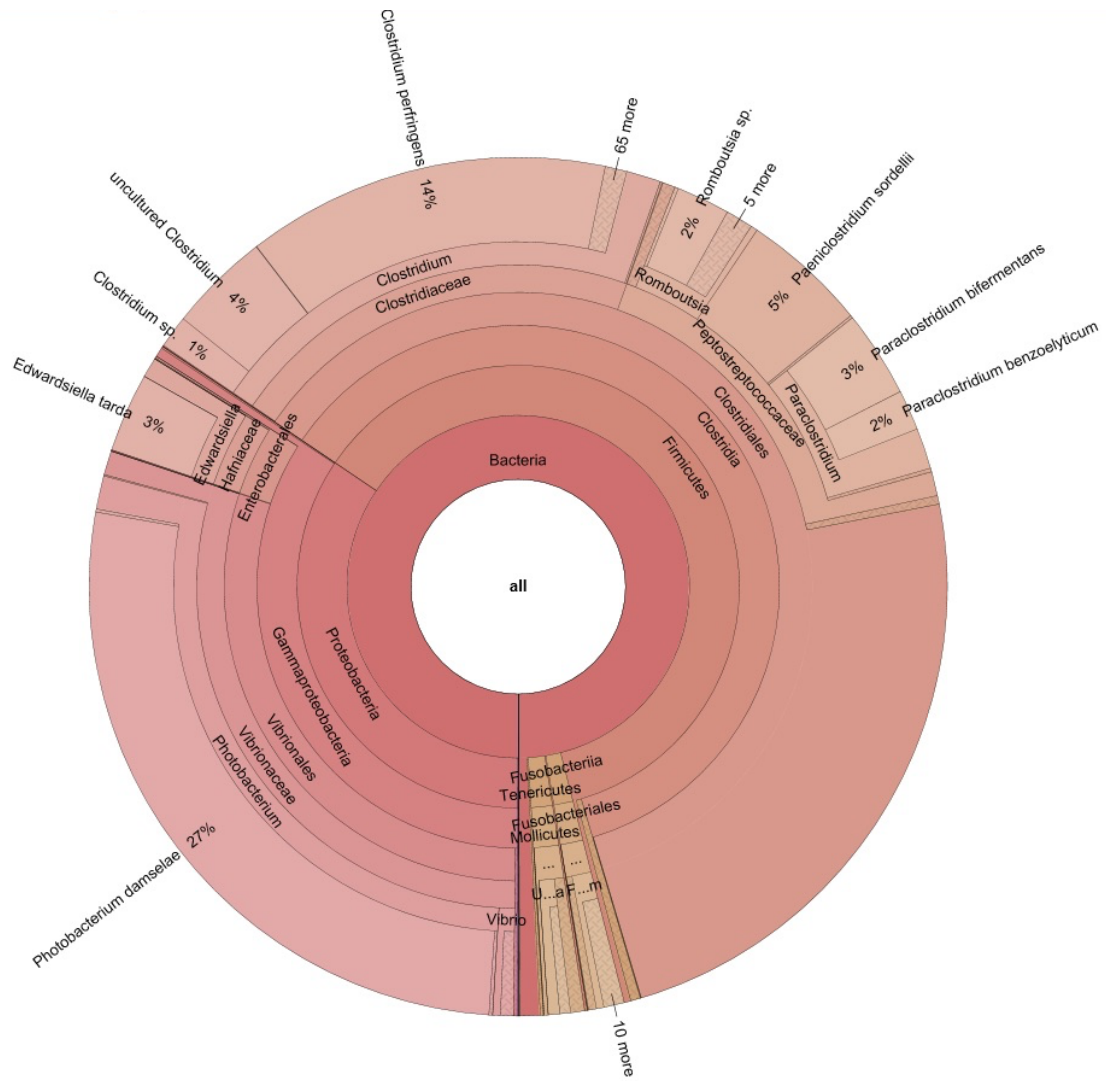




**Figure S12.** Krona chart depicting relative abundance of taxonomic groups at different hierarchical levels in the stomach sample.

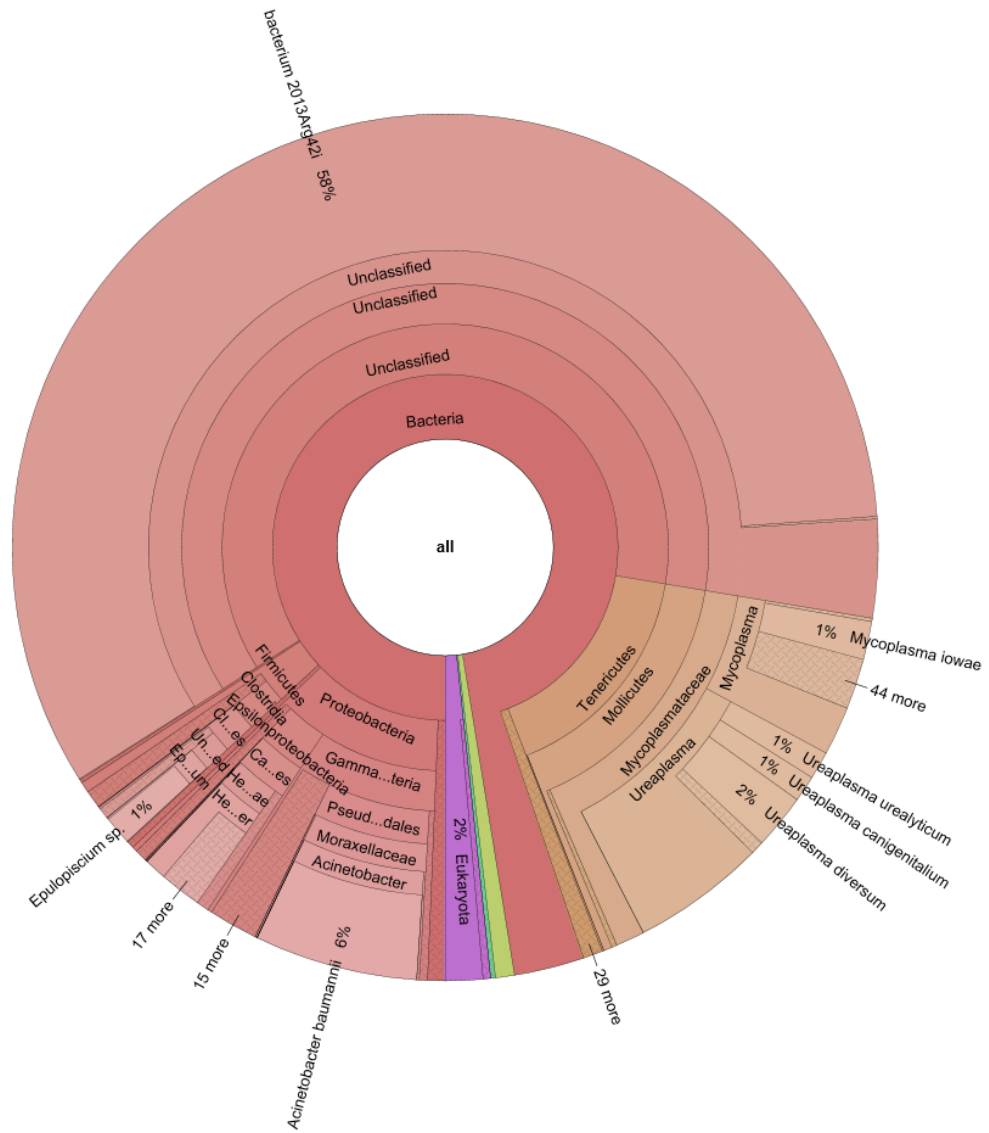




**Figure S14.** Krona chart depicting relative abundance of taxonomic groups at different hierarchical levels in the skin lesion 1 sample.

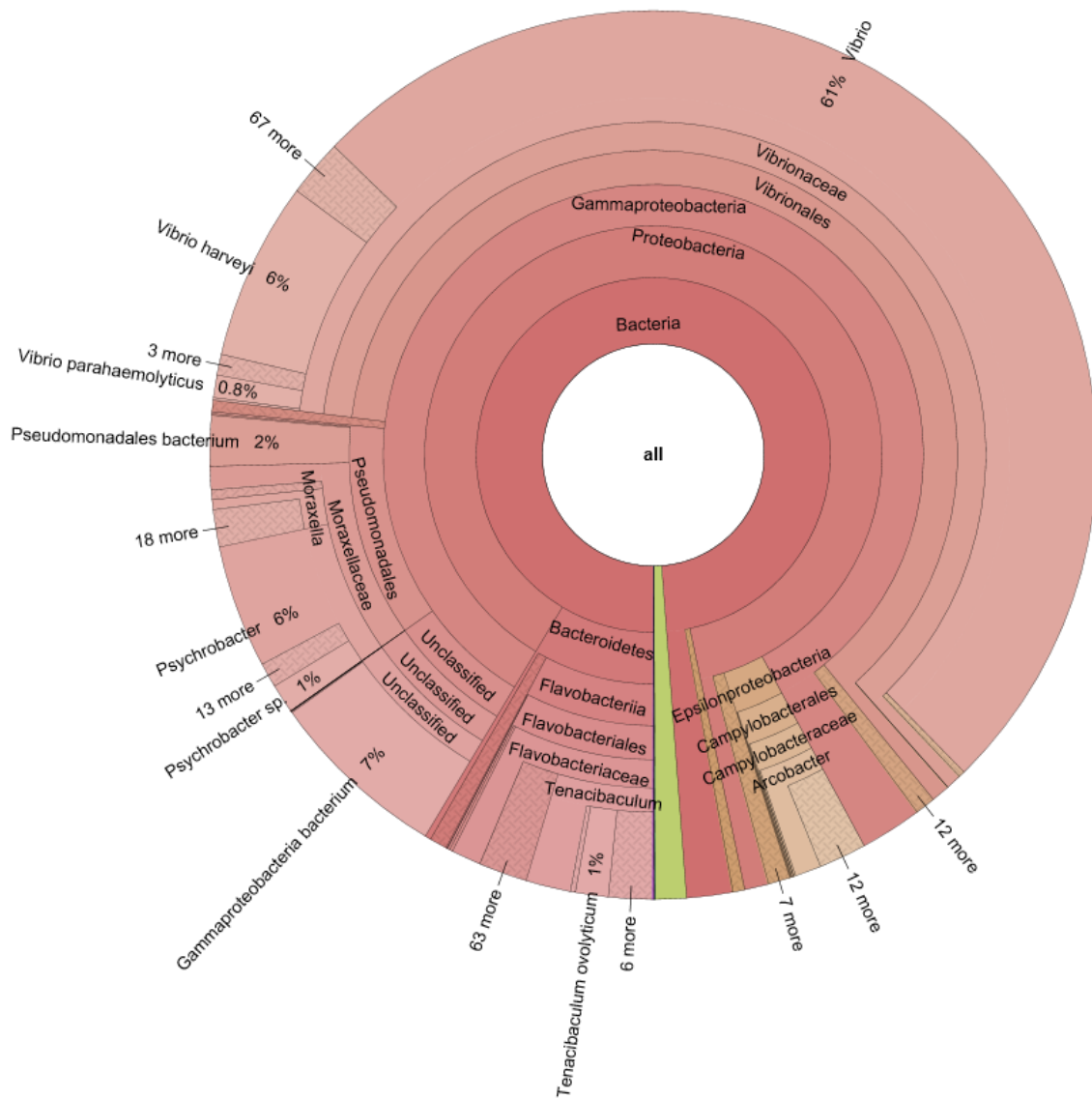


**Figure S15.** Krona chart depicting relative abundance of taxonomic groups at different hierarchical levels in the skin lesion 2 sample.

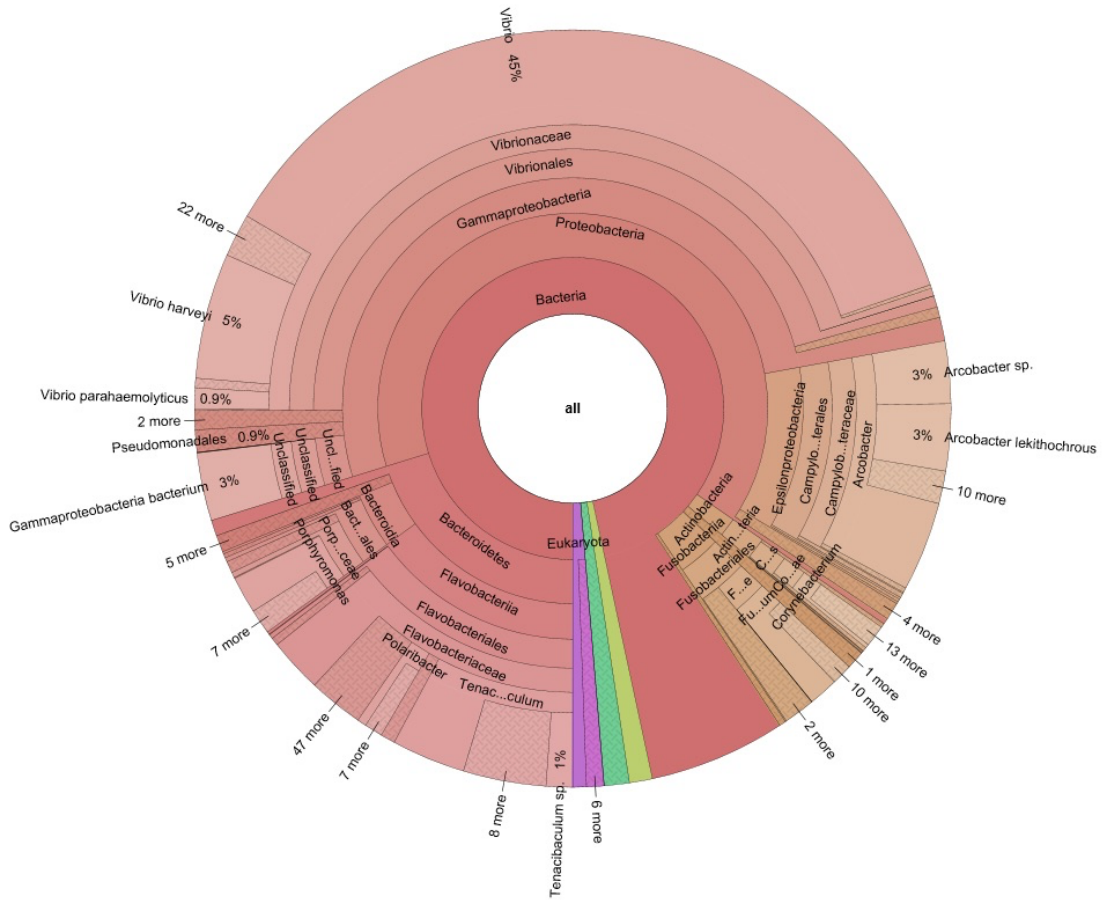


**Figure S16.** Krona chart depicting relative abundance of taxonomic groups at different hierarchical levels in the skin lesion 3 sample.

